Theses and Dissertations

August 2018

Differential Migration of CD4+ and CD8+ T Cells During an Immune Response

Jacob Parrott
University of Wisconsin-Milwaukee

Follow this and additional works at: https://dc.uwm.edu/etd

Part of the Allergy and Immunology Commons, Biology Commons, and the Cell Biology Commons

DIFFERENTIAL MIGRATION OF CD4$^+$ AND CD8$^+$ T CELLS DURING AN IMMUNE

RESPONSE

by

Jacob Parrott

A Thesis Submitted in

Partial Fulfillment of the

Requirements for the Degree of

Master of Science

in Biological Sciences

at

University of Wisconsin-Milwaukee

August 2018

ABSTRACT

DIFFERENTIAL MIGRATION OF CD4$^+$ AND CD8$^+$ T CELLS DURING AN IMMUNE RESPONSE

by

Jacob Parrott

The University of Wisconsin-Milwaukee, 2018
Under the Supervision of Professor Douglas Steeber

Lymphocyte migration is critical for recognizing pathogenic challenges in a timely manner and

generating effective, rapid immune responses. Lymphocyte numbers in secondary lymphoid

tissues such as lymph nodes are rapidly and dramatically increased during an immune response.

Lymphocytes use specific adhesion molecules and intracellular signaling cascades to migrate

and enter secondary lymphoid tissues under resting conditions. It is not clear if the same

migration and/or entry pathways are utilized when secondary lymphoid tissues are activated

during an immune response. Previous investigations in our lab have shown that T cell subtypes

display differential migration patterns to peripheral lymph nodes during an antigen-induced

immune response. Additional studies began defining the intracellular signaling cascades and

adhesion molecules that may be responsible for the observed differential migration. In the

studies presented here, inhibitors of proteins in signaling pathway(s) known to be involved in

lymphocyte adhesion and migration were used to identify the intracellular signaling cascades

responsible for the observed differential migration. Further, examination of cryosectioned

lymphoid tissue by immunofluorescence microscopy sought to elucidate involvement of the

inhibited pathways in cellular localization *in vivo* and the expression of peripheral lymph node

addressin in the recruitment of T cells to peripheral lymph nodes. Several possible intracellular

signaling pathways (PI3K and ZAP70) and L-selectin (CD62L) were eliminated as the cause of the

differential T cell migration during immune responses.

TABLE OF CONTENTS

LIST OF FIGURES

ACKNOWLEDGEMENTS

I would first like to thank Dr. Douglas Steeber for his generous mentorship and sharing his extensive knowledge of immunology during my time at University of Wisconsin-Milwaukee. I would not be the researcher I am today without his help. Further, thank you to Dr. Julie Oliver and Dr. Heather Owen for their helpful advice and ability to challenge me as a student during their time on my graduate committee. Thank you to my present and past lab mates: Joseph Skurski, Sreya Biswas, Danny Jaber, Meredith Frank, Kayla Simanek, Samer Alanani, Navjit Lehal and Jessye Hale for their help with my work and being a large part of my graduate experience. I would like to thank my parents and grandparents for supporting me during my time in graduate school (and for buying me groceries more times than I would like to admit). Finally, I would like to thank the numerous teachers, professors, coaches, and mentors I have had to this point in my life. Although sometimes unrecognized, I hope they know the generosity of their time and knowledge has gone a long way to shape their students' lives.

"Basic research is what I am doing when I don't know what I am doing"

— Wernher von Braun

Significance

Immunotherapy has garnered much interest in the therapeutic world recently. Immunotherapy, as defined by the National Cancer Institute, is a type of biological therapy that uses substances to stimulate or suppress the immune system to help the body fight cancer, infections, and other diseases. Examples of immunotherapy treatments include monoclonal antibodies (alemtuzumab, (Campath®), Nivolumab (Opdivo®)), cancer vaccines (Sipuleucel-T (Provenge®)), cytokine administration, and chimeric antigen receptor T cell (CAR-T cell) transfers. The majority of FDA approved immunotherapies are monoclonal antibody treatments for cancer therapies. However, the other areas of immunotherapy have a large amount of research interest. Specifically, CAR-T cell treatments have been of much interest lately as evidenced by the $605 million in venture capital given to companies developing CAR-T cell therapies from 2011-16 (Smith et al., 2016).

CAR-T cell treatments involve *ex vivo* expansion and/or genetic modification of tumor-specific T cells and then adoptive transfer of the cells back into the patient. This has shown some promising results (Morgan et al., 2006, Milone et al., 2009). However, the first generation of chimeric T cell therapies displayed limited efficacy in clinical trials and had issues with toxicity due to self-targeting cells (Kershaw et al., 2006, Lamers et al., 2006). The moderate efficacy has been tied to limited migration of the engineered cells (Kersahaw et al., 2006). Immunosuppressive factors, such as inhibition by indoleamine-2,3-dioxygenase, programmed cell death ligand-1, and regulatory T cells have also been suggested to play a part in reducing the efficacy of CAR-T cell treatments (Bellone and Calcinotto, 2013).

Understanding the mechanisms underlying T cell migration could help direct the CAR T cells to the desired location (tumor site in this case). Indeed, there is interest in this avenue of investigation at the preclinical stage (Dai et al., 2016). This control may not be restricted to controlling T cell migration in response to cancer. Understanding T cell migration could be useful for any type of illness or disease where a directed immune response is desired. Characterizing the mechanism for previously observed differential T cell subset migration would be a step in this direction (Grailer et al., 2010).

Related to CAR-T cell therapies, cancer vaccines seek to increase the immune system's anti-tumor immune response. Indeed, tumor-infiltrating lymphocytes are a good prognostic factor when predicting patient outcomes in diverse cancer types (Hwang et al., 2012). The most common approach is to present the patients' immune cells with tumor associated antigens (e.g. MART-1, gp100) or autologous tumor cells (Butterfield, 2015). Activation of $CD8^+$ T cells is the most common outcome sought using these methods. Vaccines that include antigen presenting cells, MHC class 1 restricted tumor-associated antigen peptides, tumor cells reengineered to express stimulatory cytokines, and oncolytic viruses are ways that have been used to activate patient-derived $CD8^+$ T cells (Butterfield, 2015).

This antigen presentation approach has been applied to autoimmune diseases in antigen-specific immunotherapy (ASI) regimens as well. The goal of ASI, like cancer vaccines, is to reprogram or otherwise reroute cells reacting to self-antigens (Pozsgay et al., 2017). Although these ideas have generated a lot of research interest, clinical trials have only shown moderate responses (Butterfield, 2015; Butterfield, 2013). Many have sought to increase the efficacy of the vaccine immunotherapies, with some promising results (Diaz et al., 2013;

Bluestone et al., 2015). Knowing how to manipulate the migration of immune cells to, or away from, disease affected area(s) could help create more efficacious immunotherapies.

Rationale

Grailer et al., in our lab, examined the subset recruitment of T and B cells based on much earlier observations (Mackay et al., 1988; Abernathy et al., 1990; Kimpton et al., 1989). These studies showed subset-specific differences in the migration of CD4$^+$ and CD8$^+$ T cells, and B cells. Previous work in our lab also found differences in lymphocyte subset migration during an immune response (Figure 1). Specifically, CD4$^+$ T cell migration to the peripheral lymph nodes (PLN) peaked earlier following immunization (Day 3) than CD8$^+$ T cell migration (Day 7; Figure 1). Attempts were made to tease apart the mechanism(s) regulating differential migration during an immune response, including examining adhesion molecules and intracellular signaling pathways known to be involved in leukocyte migration. Specifically, these studies examined the role of lymph node neovascularization, L-selectin (CD62L) function, peripheral lymph node addressin (PNAd) expression, and Gα_i-dependent chemotaxis. The use of vascular endothelial growth factor 2 receptor (VEGFR2) inhibitor SU5416 showed that neovascularization did not account for the observed differential migration. L-selectin expression was found to be necessary for mediating increased migration to the immunized PLN by adoptive transfer of L-selectin$^{-/-}$ lymphocytes into wild type mice. Interestingly, based on immunofluorescence microscopy data, PNAd expression did not increase on the vasculature of the PLN as a result of immunization. Surprisingly, despite blocking the majority of lymphocyte migration into the PLN, inhibiting Gα_i signaling in lymphocytes with pertussis toxin (PTX) did not

prevent increased migration occurring into the immunized PLN (Figure 2). These findings leave

the mechanism(s) mediating the observed differential migration unclear. A better

understanding of this process could help improve the current forms of immunotherapy.
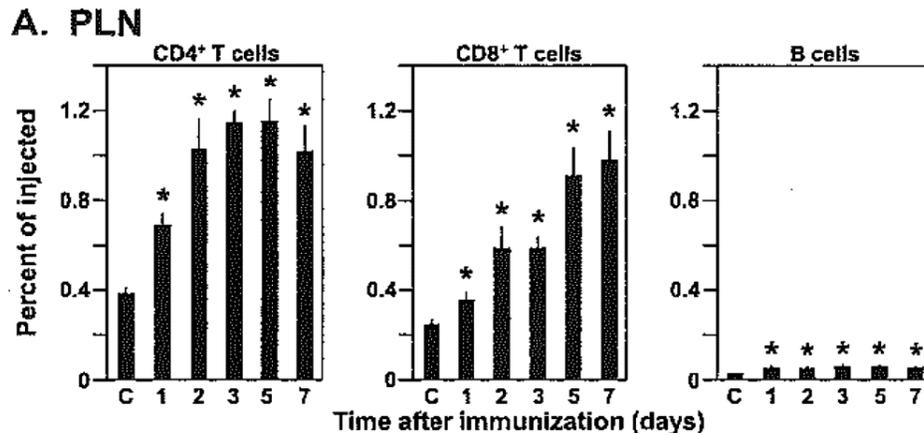
Figure 1. Immunization significantly increases the percent of injected CD4+ and CD8+ T cells that migrate to PLN. C57BL/6 splenocytes were biotinylated and injected into the lateral tail vein and allowed to migrate for 1 hour in immunized mice (days 1 thru 7). PLN were harvested, injected cells were labeled with avidin-conjugated fluorophores and subset-specific antibodies then analyzed by flow cytometry. C = unimmunized control values. *; P<0.05. Reproduced from Grailer 2010.
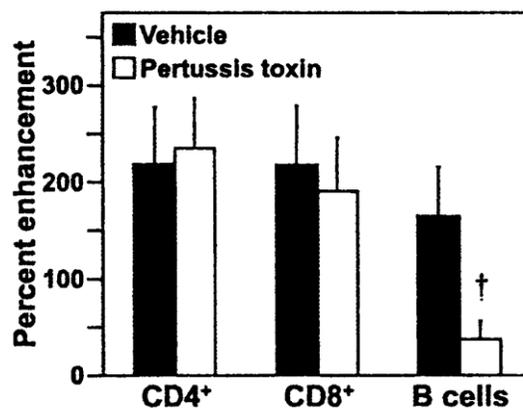
Figure 2. Inhibition of Gα$_i$ *with* **pertussis toxin (PTX) had no effect on increased recruitment of T cells following immunization**. Cells were incubated with PTX (10 µM) for 1 hour before adoptive transfer into

recipient mice that had been immunized 3 days earlier. Migration was allowed to occur for 1 hour

before PLN were harvested and analyzed as in Figure 1. [†]; P<0.05. Reproduced from Grailer 2010.

The aims and hypothesis detailed in the next section were investigated to uncover the

mechanism(s) causing differential migration between CD4^{+} and CD8^{+} T cells to secondary

lymphoid organs during an immune response.

Aims and Hypothesis

Hypothesis

Differences in migration between CD4$^+$ and CD8$^+$ T cells to secondary lymphoid tissues during an immune response are caused by differences in signaling pathway activation and not changes in adhesion molecules.

This hypothesis was tested through the following aims:

1. Determine the role of kinase signaling in mediating differential CD4$^+$/CD8$^+$ T cell migration following antigen stimulation. Migration following treatment of T cells with inhibitors against key signaling proteins including ZAP70 and phosphatidylinositol 3-kinase (PI3K) was analyzed using flow cytometry and immunofluorescence microscopy.

2. Determine the role of known adhesion molecules (i.e., L-selectin, L-selectin ligands) in mediating differential CD4$^+$/CD8$^+$ T cell migration following antigen stimulation using chimeric L-selectin fusion protein binding.

Literature Review

Lymphocytes must recirculate in the blood and/or migrate throughout the body for an efficient immune response to occur. Recirculation and migration are critical for a proper immune response because the odds of a lymphocyte recognizing a given antigen are low. For example, the odds of a naive $CD8^+$ T cell being specific for an 8 amino acid epitope on the lymphocytic choriomeningitis virus was estimated to be 1 in 200,000 (Blattman et al., 2002). Continual movement of lymphocytes through the lymphoid system via recirculation and migration must be in place to ensure that a specific lymphocyte will encounter its specific antigen. The inability to properly migrate and/or recirculate can lead to the inability of a patient to defend his or herself against immune challenges. Leukocyte adhesion deficiency (LAD) is an example of such a disorder (Harris et al., 2013). Patients with LAD are unable to clear bacterial infections, and usually succumb to the disease at a young age if no treatment is received (Tipu, 2017). An important part of this defense is the transition from the circulation in the blood to migration into the lymph nodes. Lymphocytes achieve this transition by undertaking the adhesion pathway.

The adhesion pathway for transendothelial migration has been well defined (Ley et al., 2007). There are four overlapping steps in the pathway. Transitory L-selectin binding to PNAd is the first step. This transitory binding allows the L-selectin$^+$ cells to roll along the cell membranes of PNAd expressing endothelial cells. Secondly, integrins on the rolling cells are activated by chemokines decorated on the cell membranes of the PNAd$^+$ cells. The integrins go from an inactive state to an active state when the appropriate chemokine(s) are bound. In the third

step, the active integrins then bind to their appropriate ligand, primarily intercellular adhesion molecule-1 (ICAM-1) in the peripheral lymph nodes, and stop the cell in what is called firm adhesion. Finally, cells undergo transendothelial migration (also called extravasation or diapedesis), exiting the blood stream and entering the tissue. The chemokines that activate the integrins can vary depending on the tissue and immune status. During homeostasis, the chemokines CCL19 and CCL21 are the dominant chemokines causing integrin activation. There are several other chemokines that are thought to be important in the direction of immune cells to lymphoid organs and/or sites of inflammation (Luster et al., 2005).

L-selectin's role in the adhesion cascade should be emphasized. Indeed, without L-selectin expression there is a 70-90% reduction in extravasation into lymph nodes by lymphocytes (Steeber et al., 1996). L-, P-, and E-selectin make up the selectin family. L-selectin is expressed on all leukocytes, E-selectin is expressed on inflamed endothelial cells (along with some P-selectin), and P-selectin is expressed on activated platelets (Grailer et al., 2009). The selectins are characterized by a calcium-dependent lectin domain, an epidermal growth factor-like domain, and short consensus repeat domains (Grailer et al., 2009). L-selectin recognizes the 6-sulfo sialyl Lewis x (sLex) domain that is expressed in PNAd to mediate its binding (Rosen, 2004). It is of note that the sLex domain is usually identified by the MECA-79 antibody (Rosen, 2004).

Finally, as it pertains to this work, L-selectin contains a membrane proximal cleavage site that is not found in the other selectins (Chen et al., 1995; Grailer et al., 2009). Cleavage of L-selectin is a necessary process for cells to maintain an appropriate amount of surface-bound L-

selectin. Blocking L-selectin cleavage results in an increase in L-selectin expression levels that alter the normal migration patterns of leukocytes (Venturi et al., 2003).

Chemokines, shortened from chemotactic cytokines, are proteins used to control the migration of immune cells (Griffith et al., 2014). Chemokines are 8-12kDa proteins that are categorized by the position of conserved N-terminus cysteine residues (Turner et al., 2014). The four major subfamilies of chemokines are CC, CXC, C, and CX3C that bind to their respective receptors (e.g., CCR, CXCR) (Turner et al., 2014). The chemokines that are most important in lymphocyte migration, and therefore most commonly studied, are the CC and CXC chemokines. Indeed, CCL21 is an example of a chemokine important for regulating homeostatic lymphocyte migration into lymphoid tissues. Further, CCR7, and its ligands CCL21/19, regulate the majority of naïve T cell migration. CXCR4 and CXCL12 is another receptor-ligand pair that directs migration of naive T cells, albeit to a lesser extent than the CCR7-CCL19/21 paring (Scimone et al., 2004). These chemokines, along with the adhesion pathway described above, allow lymphocytes to recirculate from the blood to a secondary lymphoid organ and then back to the blood every 10 to 20 hours (Mandl et al., 2012).

G proteins are heterotrimeric guanine nucleotide binding regulatory proteins that are responsible for relaying intracellular signals from G-protein coupled receptors (GPCRs) on the cell membrane (Syrovatkina et al., 2016). They have been extensively studied and the majority of the signaling pathways utilized by GPCRs have been elucidated. GPCRs are of particular interest in immunology because of their importance regulating migration of leukocytes (Griffith et al., 2014). CCR7, described above, is an example of a GPCR. The G proteins responsible for the intracellular signaling activity of GPCR are composed of α, β, and γ subunits (Syrovatkina et

al., 2016). The α subunit is known to dissociate from the GPCR as an individual subunit, but the β and γ subunits are tightly associated. These two subunits are considered as one unit when examining the signaling pathways used by GPCRs. G proteins can be divided into four families based on the sequence similarity of the α subunit. The families are $G\alpha_s$, $G\alpha_i$, $G\alpha_q$, and $G\alpha_{12}$ (Syrovatkina et al., 2016). The $G\alpha_i$ family is the most diverse family of G proteins and are the most relevant for signaling in leukocytes (Griffith et al., 2014, Syrovatkina et al., 2016).

The receptor part of the GPCR consists of seven-transmembrane helices. These receptors, in conjunction with the associated G proteins, transmit the signal from outside to inside the cell following chemokine binding. Interestingly, CD4^{+} and CD8^{+} T cells have different transit times through lymph nodes (Mandl et al, 2012). Mandl et al., investigated the cell surface molecules that could account for the transit time difference, and found that CCR7 was about two-fold higher expressed on CD4^{+} T cells compared to CD8^{+} T cells. However, they were not able to conclude that the increase in CCR7 expression accounted for the transit time difference.

The GPCR $\beta\gamma$ subunit has been shown to interact with phosphoinositide 3-kinase (PI3K) to mediate leukocyte migration in response to chemokines (among other chemoattractants) (Ward et al., 2011). Indeed, the PI3K p100δ subunit has been shown to be necessary for migratory responses to antigen (Jarmin et al., 2008). Interestingly, there seems to be a preference for different catalytic subunits of PI3K based on the signal a lymphocyte receives (Thomas et al., 2008). PI3K has several functions in the cell, but the most relevant for lymphocyte migration is its role in actin dynamics (Sinclair et al., 2008, Martin et al., 2008,

Nombela-Arrieta et al., 2007). Further, the p100δ subunit of PI3K controls CD62L expression through mitogen activated protein kinases (MAPKs) and the mammalian target of rapamycin (mTOR) pathway (Sinclair et al., 2008). The PI3K pathway connects with the mTOR pathway to mediate lymphocyte differentiation and migration (Powell et al., 2012). Signals that enter the mTOR pathway can travel through mTOR Complex 1 (mTORC1) or mTOR Complex 2 (mTORC2) (Pollizzi and Powell, 2015). Signaling through PI3K and mTOR has also been found to be at a crossroads between T cell metabolism and migration (Sinclair et al., 2008).

Hypoxia-inducible factor 1 (HIF-1) has also been shown to be required for proper CD8^{+} T cell immune response and is dependent on mTORC1 function (Finlay et al., 2012). Specifically, HIF-1 knockout results in CD8^{+} T cells maintaining CCR7, among other chemokine receptors, and L-selectin expression following activation (Finlay et al., 2012). This finding was the result of dysregulated glucose uptake by the HIF-1 knockout cells. The maintained expression of these molecules was recapitulated by activating CD8^{+} T cells in a low glucose environment (Finlay et al., 2012). These results implicate metabolism, and glucose availability, as important regulators of changes in migration patterns of CD8^{+} T cells during an immune response.

Rapamycin inhibition of mTOR also results in CD8^{+} T cells maintaining high levels of CCR7 and CD62L expression after activation (Sinclair et al., 2008). Activated CD8^{+} T cells usually have low expression of CCR7 and CD62L so that they break out of homeostatic recirculation pathways. These activated cells then search for inflammatory sites to perform their cytotoxic effector functions. Indeed, rapamycin treatment of IL-2-stimulated CD8^{+} T cells caused an increase in the number of CD8^{+} T cells found in the lymph nodes and spleen (Sinclair et al., 2008). 3-phosphoinositide-dependent kinase 1 (PDK1) is a kinase that binds phosphoinositide

(3,4,5)-triphosphate (PIP3) that can be released during cell activation (Waugh et al., 2009).

PDK1 is necessary to then signal downstream to regulate trafficking of CD8$^+$ T cells, in the same

way as PI3K regulation of the mTOR pathway, during homeostasis and inflammatory responses

(Waugh et al., 2009).

ZAP70 is an intracellular protein kinase that binds to the cytoplasmic domain of the T

cell receptor (TCR) and is phosphorylated when the TCR is engaged by an appropriate major

histocompatibility complex (MHC) molecule loaded with peptide (Chan et al., 1992). ZAP70 is

necessary for proper immune function, and one form of severe combined immunodeficiency

results when ZAP70 is non-functional (Chan et al., 1994). ZAP70 function has also been

implicated in T cell migration (Lin et al., 2010). Specifically, Lin et al., showed that inhibiting

ZAP70 affected the directionality of T cell movement *in vitro*. They also showed that ZAP70

interacted with integrin talin domains but could not show that ZAP70 phosphorylated these

domains. Talin domains associate with cytoplasmic portions of integrins after they are activated

by GPCR signaling (Critchley, 2004). This association allows the proper activation of integrins

(Boettner and Van Aelst, 2009). Indeed, lack of adhesion is observed when talin is not present

in cells (Priddle et al., 1998). These results correlate ZAP70 function and integrin activation

which, as has been discussed above, is a critical step for migration of T cells. Part of the present

work was to investigate the role of ZAP70 during *in vivo* migration of T cells during an immune

response.

Wortmannin is a metabolite of the plant pathogen *Penicillium funiculosum* that has

been used since the early 1990's as a non-selective covalent inhibitor of PI3Ks (Yano et al.,

1993). The metabolite has been shown to be a more potent inhibitor of PI3Ks than the first

synthetic PI3K inhibitor LY294002 (2-4 nM versus 0.5-1 μM respectively). Both of these

inhibitors, as well as other 'first generation' analogues, were examined in clinical trials after

PI3K signaling was implicated in cancer (Westin et al., 2014). However, these first generation

PI3K inhibitors were not very successful in trials as intolerable off-target effects and/or

solubility issues were uncovered (Yap et al., 2008). Both inhibitors have continued to be widely

used for basic research nevertheless (especially where specificity is not required). Further,

wortmannin has been used by many groups to study the role of PI3K signaling in immune cell

migration (Dey et al., 2010, Wain et al., 2002, Reif et al., 2004).

Piceatannol, the other inhibitor used in the present work, is an analogue of revesterol,

formed by addition of a hydroxyl group by cytochrome P450 during metabolism, that retains

revesterol's antiproliferative and antioxidant effects (Murias et al., 2005, Wolter et al., 2002).

Piceatannol has also been shown to inhibit ZAP70 signaling (Soede et al., 1998). This inhibition

has been shown to reduce effector protein secretion and expression *in vitro* (Kim et al., 2015).

Piceatannol inhibition of ZAP70 has also been shown to interfere with the directionality of T cell

migration to cancer spheroids in a 3-D culture system (Lin et al., 2010). Further, previous

studies in the Steeber lab described a role for ZAP70 in migration of T cells out of the high

endothelial venules (HEV) and into the PLN (Subramanian et al, 2012).

Experimental Methods

Mice

C57BL/6 mice (The Jackson Laboratory, Bar Harbor, ME) were housed and bred in pathogen-free, climate-controlled conditions according to the Institutional Animal Care and Use Committee at the University of Wisconsin-Milwaukee. Both male and female mice aged between 8 and 12 weeks old were used.

Immunization

Alum-precipitated mariculture Keyhole Limpet Hemocyanin (mcKLH) (Pierce, Waltham, MA) was used to create a robust immune response in the mice. The mcKLH (10 mg/mL stock concentration) and alum (Pierce, Waltham, MA) was combined in a 1:1 ratio and mixed with a magnetic stir rod for 30 minutes at room temperature prior to use. 125 µg of the mcKLH-alum in 25 µL volume was injected into the hind and fore footpads on one side of the recipient mice. 25 µL of PBS (0.15 M NaCl, 155 mM Na_2HPO_4, 46.6 µM $Na_2H_2PO_4$ monohydrate) was injected into the opposite hind and fore footpads of the mice as a control for injection. The immune response was allowed to progress for 3 to 7 days. Cells prepared as described below were adoptively transferred into the immunized mice by lateral tail vein injection.

Adoptive Transfer Assay

Donor spleens from C57BL/6 mice were dissociated using 27 gauge needles and splenocytes were collected after being filtered through a 70 µm nylon mesh. Erythrocytes were lysed with a 0.15 M ammonium chloride solution. Cells were counted with a hemacytometer

and then 25×10^6 cells/mL were labeled with EZ-Link Sulfo-NHS-LC-Biotin (Thermo Scientific, Waltham, MA) at a final concentration of 80 µg/mL. Alternatively, 12×10^6 cells/mL were labeled with carboxyfluorescein succinimidyl ester (CFSE) (Invitrogen, Carlsbad, CA) at a final concentration of 0.5 µM. CFSE labeled or biotinylated cells were incubated with pertussis toxin at 100 ng/mL (List Biological Laboratories, Campbell, CA), piceatannol at 10 µM (Enzo Life Sciences, Farmingdale, NY), or wortmannin at 100 nM (Upstate Cell Signaling, Lake Placid, NY) for 1-hour inhibitor transfer assays. Labeled cells were washed 3 times in PBS and injected i.v. through the lateral tail vein of recipient mice. Cells were allowed to migrate for 5 minutes or 1 hour before the animal was euthanized. Spleen and popliteal and axillary lymph nodes were dissected from the recipient mice. The popliteal and axillary lymph nodes were combined, and single-cell preparations were made from all tissues as described above for the donor cells. Lymph nodes, spleen, and pre-injection cells were labeled with avidin-PE (SouthernBiotech, Birmingham, AL), anti-CD4 Alexa Fluor® 647, anti-CD8 Alexa Fluor® 647 (both BD Bioscience, San Jose, CA), or isotype control antibodies (SouthernBiotech). Anti-CD4 Alexa Fluor® 647 was used at 1:1000 dilution and anti-CD8 Alexa Fluor® 647 was used at 1:250. Cells with the light scattering properties of mononuclear cells were gated, and 500-2000 adoptively transferred and labeled cells were collected per sample using a FACSCalibur flow cytometer (BD Biosciences, San Jose, CA). The percent of injected cells was calculated by dividing the number of labeled subtype cells ($CD4^+$ or $CD8^+$ T cells) found in a tissue (e.g. spleen or PLN) by the corresponding number of subtype cells injected. R_o/R_i was calculated by dividing the ratio of inhibitor vs. control treated cells recovered (R_o) by the ratio of inhibitor vs. control treated cells injected (R_i) ((inhibitor vs. control cells recovered) / (inhibitor vs. control cells injected)).

Immunofluorescence Microscopy

Tissues were harvested from donor mice, placed in a base mold containing Optimal

Cutting Temperature (OCT) tissue freezing medium (Sakura FineTek, Torrance, CA) and frozen

on dry ice. Tissues were then stored at -20°C until use. Tissues were sectioned with a Leica

CM1900 cryostat and collected on Superfrost Plus® microscope slides (VWR International, West

Chester, PA). Sections were stored at -20°C until use. Slides were allowed to warm to room

temperature, fixed in cold (-20°C) acetone, and allowed to air dry. Sections were encircled using

a hydrophobic pen (PAP pen; Biotium, Freemont, CA) before being rehydrated with PBS

containing 2% (v/v) horse serum (wash buffer) and blocked with 2% normal goat serum in PBS.

Tissues were then labeled with anti-CD4 or anti-CD8 Alexa Fluor® 647-conjugated antibodies,

MECA-79 culture supernatant (American Type Culture Collection, Manassas, VA), or isotype

control antibodies, as specified, in the dark. MECA-79 labeling was detected using DyLight 405-

conjugated AffiniPure goat-anti-rat IgM antibody (Jackson Immuno Research, West Grove, PA).

Biotin^{+} cells were revealed by using avidin conjugated with TRITC (Jackson Immuno Research,

West Grove, PA). Sections were washed with wash buffer at room temperature between

staining steps, and with PBS at room temperature after all staining steps were completed.

Finally, slides were mounted under glass coverslips with ProLong™ Gold antifade mountant

(Invitrogen, Eugene, Oregon) and imaged using a Nikon Eclipse TE-2000U inverted fluorescence

microscope (Nikon, Melville, New York). Images were captured with a CoolSNAP ES camera

(Photometrics, Tucson, Arizona) and analyzed using MetaVue software (Molecular Devices,

Sunnyvale, California). Cells per 1000 μm^2 HEV was calculated by adding all of the biotin^{+} cells

counted in the HEV field and then dividing by the total μm^2 of HEV found in that field. Total μm^2 of HEV was calculated using the measure tool in MetaVue.

Statistics

Data are presented as the mean ± SEM unless stated otherwise. Significant differences between sample means was determined by Student's *t* test. A *p* value of <0.05 was considered statistically significant.

Results

Mice were immunized with mcKLH-alum in the hind and fore footpads on one side and PBS on the contralateral side and allowed to respond for 3 or 7 days. Figure 3 shows that the immunization protocol described significantly increased the cellularity of the stimulated PLN compared to the contralateral control tissues by day 3. Additional increase in cellularity of the immunized lymph nodes was observed at day 7 (data not shown). These data further show that the immunization protocol elicited an immune response only on the immunized side of the animal. Therefore, this protocol was used to examine differences in lymphocyte migration for all future lymphocyte transfer assays.
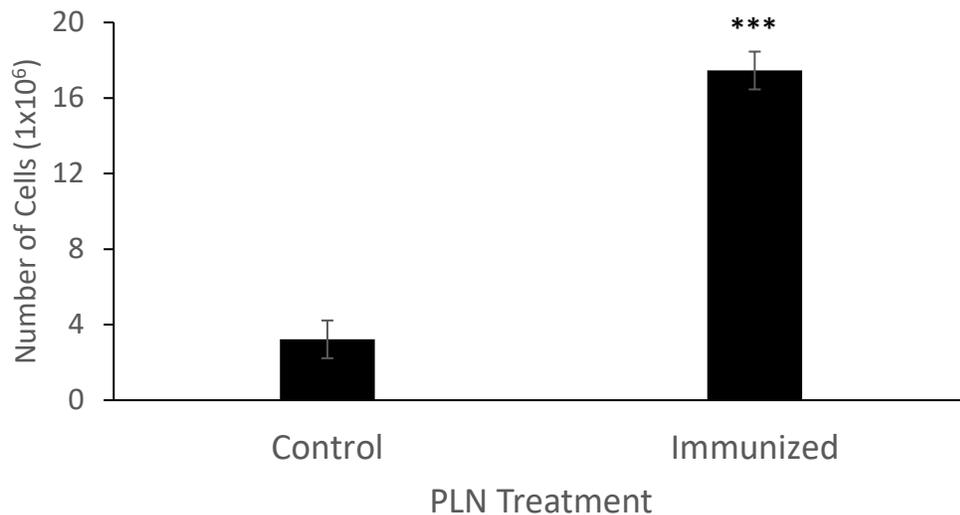
Figure 3. Immunized PLN have significantly increased cellularity compared to control PLN. Mice were immunized with mcKLH-alum in the hind and fore paw on one side and PBS on the contralateral side. Mice were allowed to respond for 3 days before PLN were removed. Values represent the mean ± SEM total cell counts from at least 4 independent experiments. ***, $P<0.001$

Figure 4 shows flow cytometry data from a control experiment where biotinylated and CFSE-labeled cells were untreated, mixed together and allowed to migrate for 1 hour in a recipient mouse. The left panel in Figure 4A shows a representative example of how biotinylated CD4^{+} T cells were gated (R2) while gating of CFSE-labeled CD4^{+} T cells (R3) is shown in the right panel. CD8^{+} T cells were analyzed similarly (data not shown). Figure 4 shows that labeling with CFSE or biotin does not affect migration of CD4^{+} or CD8^{+} T cells relative to one another as indicated by a R_o/R_i ratio of 1. Further, flow cytometry analysis showed that CCR7 and CD62L expression were not significantly changed at the time the cells were injected due to cell handling and/or labeling (data not shown).

Pertussis toxin (PTX) is known to inhibit the $G\alpha_i$ subunit of the GPCR, and therefore inhibits $G\alpha_i$–dependent migration. Specifically, lymphocyte responses to CCL21/19 (as detailed above) are dependent on $G\alpha_i$ signaling. Figure 5 shows that treatment with PTX virtually eliminated migration to PLN for both CD4^{+} and CD8^{+} T cells in 1 hour adoptive transfer experiments. This serves as a positive control for other inhibitor transfer assays and indicates that this assay can detect differences in migration for both CD4^{+} and CD8^{+} T cells.

A

B
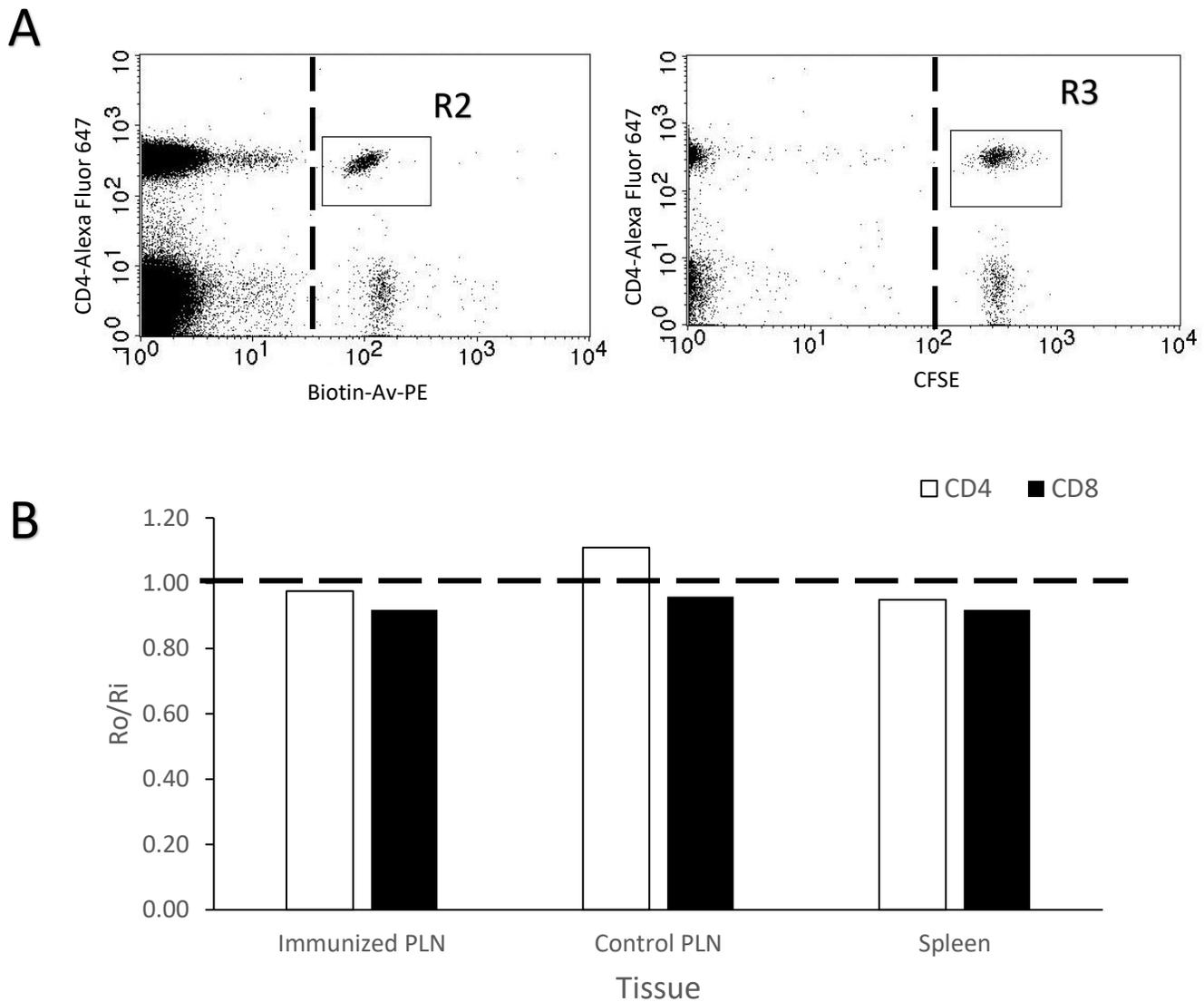
Figure 4. Biotin and CFSE labeling procedures do not affect the migratory ability of T cells. Equal numbers of biotin- and CFSE-labeled cells (36x10^6 total cells) were injected into the lateral tail vein of a C57BL/6 mouse immunized three days prior and allowed to migrate for 1 hour. A) Left panel: Biotin-Avidin-PE-labeled CD4$^+$ T cells are contained in the R2 gate; Right panel: CFSE-labeled CD4$^+$ T cells are contained in the R3 gate. The vertical dashed line in each panel indicates transferred biotin$^+$ or CFSE$^+$ cells that were recovered. B) The ratio of CFSE- to biotin-labeled cells recovered in the organ (Ro) was divided by the ratio of CFSE- to biotin-labeled cells injected (Ri) to normalize migration results as described in the methods section. The horizontal dashed line indicates equal migration of biotin- and

CFSE-labeled cells (Ro/Ri = 1). A value over 1 indicates increased migration of the CFSE-labeled cells, and a value under 1 indicates decreased migration. In this example both groups of cells were untreated and thus a result near 1 is expected. Results are from 1 experiment.
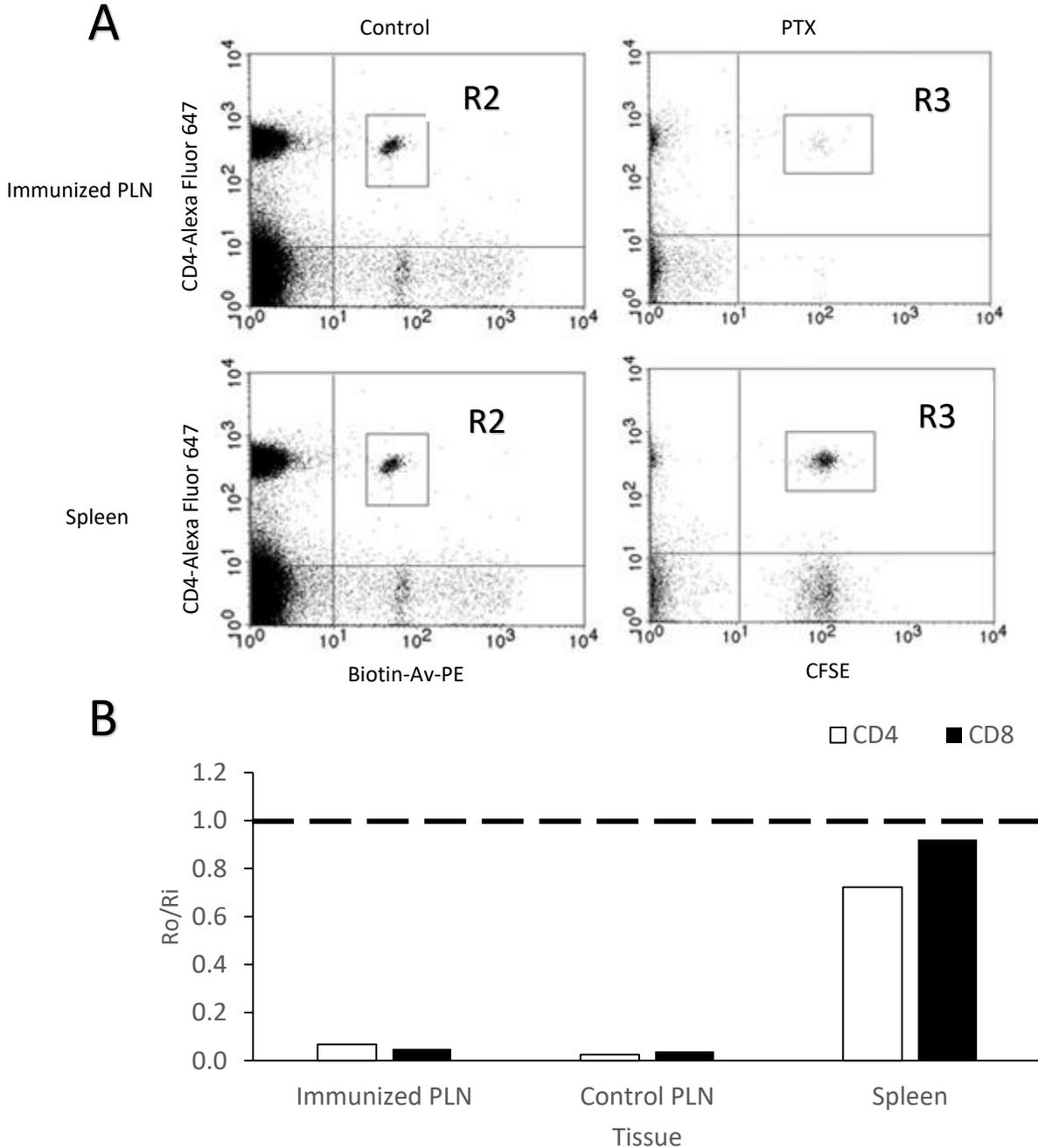
Figure 5. PTX treatment reduces the migration of T cells to PLN. Cells were labeled with either biotin or CFSE. CFSE-labeled cells were treated with PTX (100ng/mL) for 1 hour and then mixed with an equal

number of vehicle-treated (control) biotin-labeled cells. Combined cells were injected into the lateral tail

vein of day 3 immunized recipient mice and allowed to migrate for 1 hour. A) Top Left: Control-treated

CD4+ T cells (R2) in the immunized PLN; Top Right: Pertussis toxin (PTX)-treated CD4+ T cells (R3) in the

immunized PLN; Bottom Left: Control-treated CD4+ T cells in the spleen; Bottom Right: PTX-treated

labeled CD4+ T cells in the spleen. B) Recovered cells were compared by the Ro/Ri ratio as above. Results

are from 1 experiment.
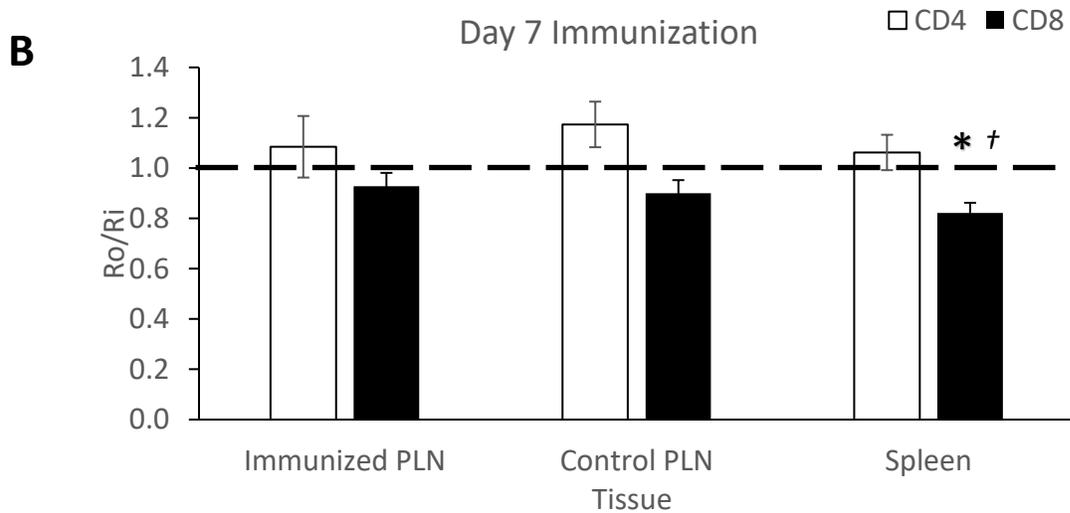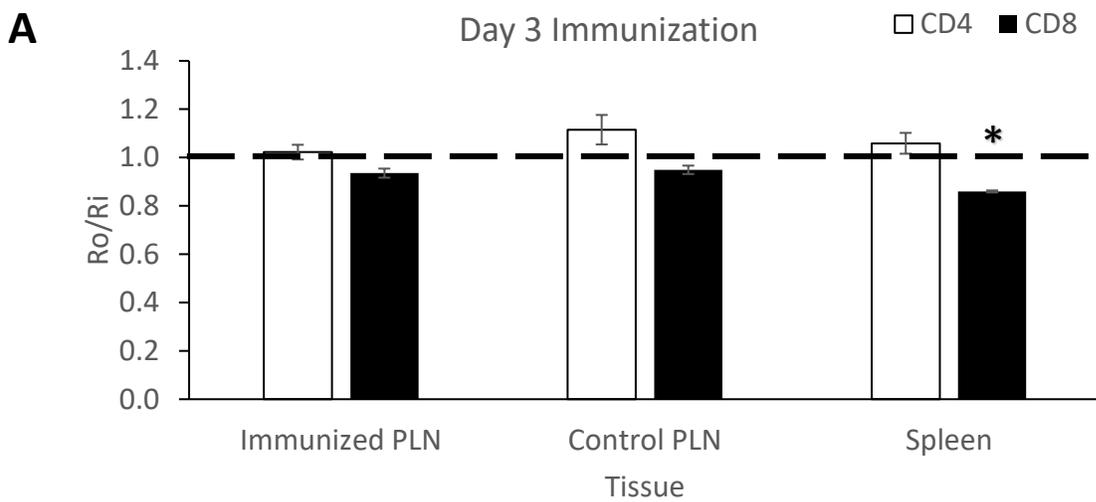
Figure 6. Piceatannol treatment did not significantly affect T cell migration to the PLN. Piceatannol (10μM) was incubated with splenocytes for 1 hour before being adoptively transferred to recipient mice that had been immunized 3 days (A) or 7 days (B) prior and allowed to migrate for 1 hour. Recovered cells were compared by the Ro/Ri ratio as above. Bars represent the mean ± SEM of results from 3 independent experiments. * significantly different from control-treated cells; [†] significantly different from CD4^{+} T cells; $p < 0.05$.

Adoptive transfer assays using piceatannol-treated cells to inhibit ZAP70 function were performed and analyzed in the same way as the control and PTX treatment experiments described above. Recipient mice were immunized 3 or 7 days before adoptive transfer of piceatannol- or vehicle-treated control cells. Figure 6 shows that piceatannol treatment did not have a significant effect on 1 hour CD4^{+} or CD8^{+} T cell migration to control or immunized PLN. However, CD8^{+} but not CD4^{+} T cell migration was significantly reduced to the spleen for both day 3 and 7 transfers. This suggests that signaling through ZAP70 is dispensable for migration to PLNs during an immune response.

A

B
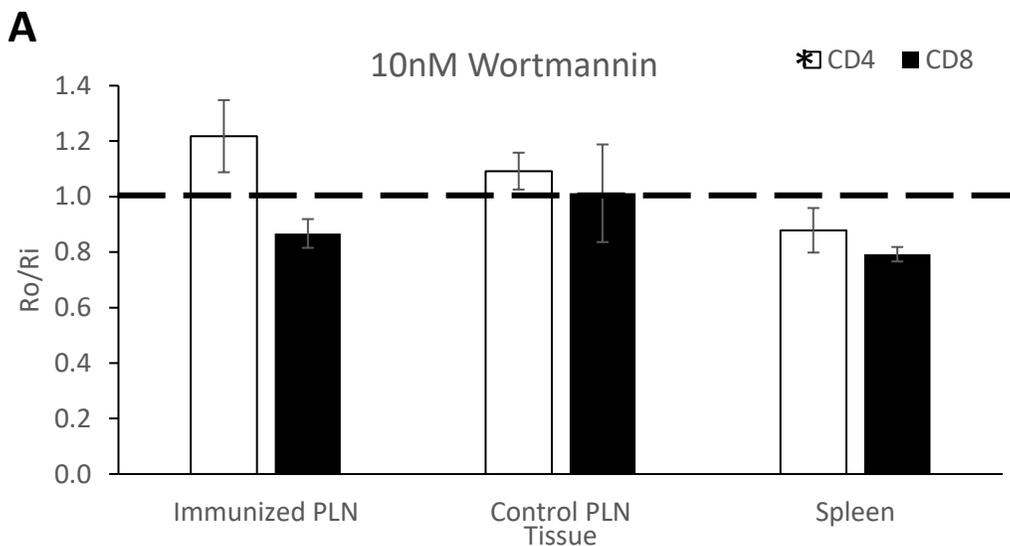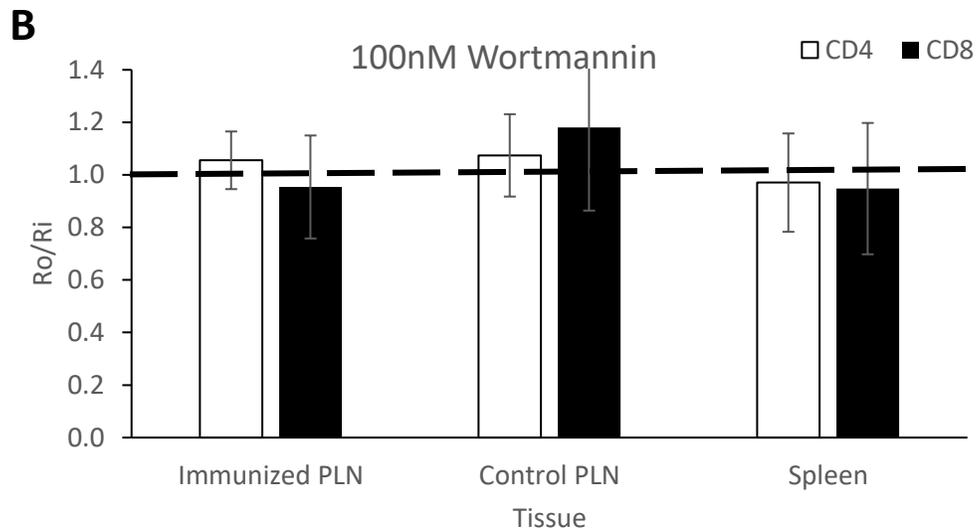
Figure 7. Wortmannin treatment did not significantly affect T cell migration to the PLN. A) Splenocytes

were prepared, treated with 10nM Wortmannin (A), or 100nM Wortmannin (B) and adoptively

transferred into recipient mice that had been immunized 3 days prior. Bars represent the mean ± SEM of

results from 3 independent experiments. * significantly different from control-treated cells; $p < 0.05$.

Additional adoptive transfer experiments were performed treating cells with

wortmannin (10 or 100 nM) to inhibit PI3K activity. Similar to treatment with piceatannol

treatment, neither concentration of wortmannin significantly reduced migration to control or

immunized PLN after 1 hour of migration (Figure 7A-B). While a slight reduction in CD8^{+} T cell

migration to the spleen was found with the 10 nM wortmannin treatment, this was not

observed at the higher concentration. These results indicate that the PI3K pathway is not

required for migration to the PLN under resting or immunized conditions.

Figures 6 and 7 show that ZAP70 and PI3K signaling are not required for migration of

CD4^{+} or CD8^{+} T cells to the PLN during an immune response. Although there was no significant

effect on the total number of CD4^{+} or CD8^{+} T cells migrating to the PLN, the inhibition of ZAP70

or PI3K pathways could cause improper localization of treated T cells in the PLN or spleen. To

examine this possibility, immunofluorescence microscopy of sectioned lymphoid tissues following adoptive transfer of inhibitor-treated cells was used.

Cells were labeled, treated, and injected as described for Figures 4-7, but the PLN and spleen were frozen, sectioned, and examined by immunofluorescence microscopy instead of flow cytometry. Figure 8A shows a representative image of labeled transferred cells in a T cell zone of the spleen. The image is of piceatannol-treated cells in the spleen but transfer of wortmannin-treated cells produced similar images. T cell zones were identified based on CD4 or CD8 antibody labeling and outlined using MetaVue software. Biotin$^+$ and CFSE$^+$ cells were counted as "In" if they were inside the outlined area and counted as "Out" if they were outside of the area. The In and Out counts were used to calculate the In/Out ratio for each treatment and cell type. Figures 8B and 8C show that neither wortmannin nor piceatannol prevented CD4$^+$ or CD8$^+$ T cell migration to the splenic T cell zones after 1 hour of migration. Interestingly, both the CD4$^+$ and CD8$^+$ wortmannin-treated T cells did have higher In/Out ratios compared to corresponding control cells in the single experiment.

In another set of experiments, the effects of piceatannol treatment on T cell migration to and within the PLN were examined. Piceatannol treatment of cells and 1-hour adoptive transfer was performed as above. The control and immunized PLN were harvested and sectioned as described. MECA-79 culture supernatant was used to label the HEV, anti-CD4 or CD8 antibodies were used to visualize the T cell subtypes, and avidin-biotin or CFSE labeling was used to label the treated (CFSE$^+$) or untreated (biotin$^+$) cells. Figures 9A and 9B show that CD4$^+$ or CD8$^+$ T cells treated with piceatannol exited the HEV and migrated similarly to untreated CD4$^+$ or CD8$^+$ T cells. This was determined by observing that the treated, transferred CD4$^+$ or

CD8^{+} T cells were not contained in the HEV, and that they localized to similar areas as the untreated T cells did in the PLN. Comparison of the immunized PLN images (Figures 9A and 9B) to the control PLN (images not shown) showed that the CD4^{+} and CD8^{+} T cells exited the HEV and localized comparably to the control PLN. In summary, wortmannin or piceatannol treatment of the cells did not affect the localization of CD4^{+} or CD8^{+} T cells within the PLNs or spleen. We next assayed for differences in CD4^{+} and CD8^{+} T cell transmigration across the HEV during short-term migration to determine whether this could account for the observed differential migration.

A

B

C
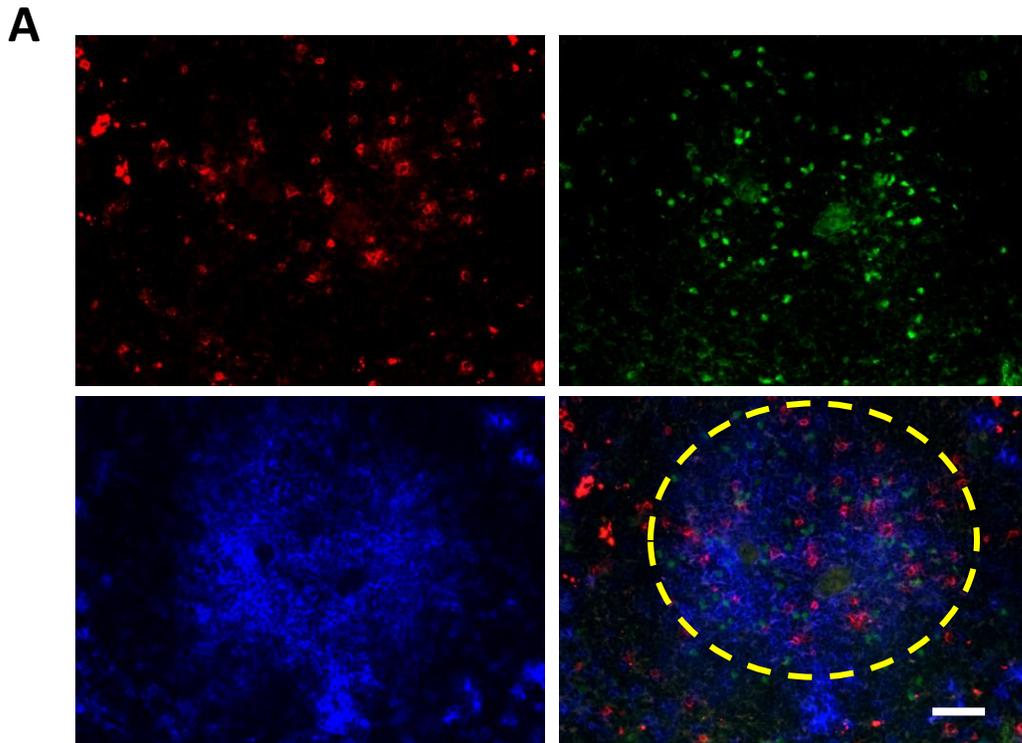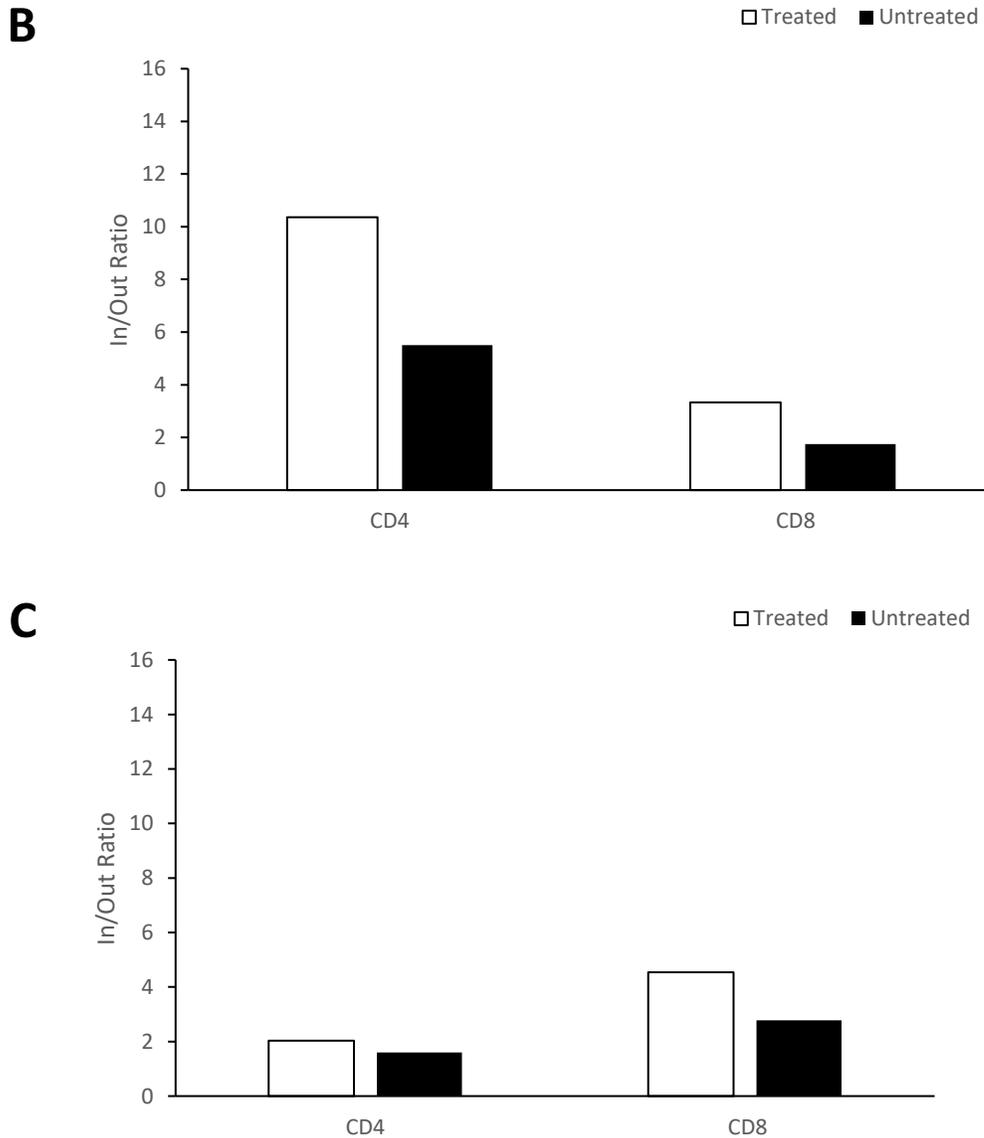
Figure 8. Neither wortmannin nor piceatannol treatment significantly affected the localization of CD4+ or CD8+ T cells to the T cell zone in the spleen. A) Representative image of a splenic T cell zone from a piceatannol treatment experiment. Single color images were overlaid to create the final image (bottom-right) used to calculate In/Out ratios (Blue=CD8+ T cells, Green= CFSE+ cells (treated), Red= biotin+ cells (untreated)). Thin arrows indicate the presence of transferred biotin+ cells, and thick arrows indicate transferred CFSE+ cells. Yellow circle indicates what was considered the T cell zone. Scale bar represents

50 µm. B) In/Out Ratio of wortmannin treated and untreated CD4$^+$ or CD8$^+$ T cells. C) In/Out Ratio of

piceatannol treated or untreated CD4$^+$ or CD8$^+$ T cells. Results are from 1 experiment.
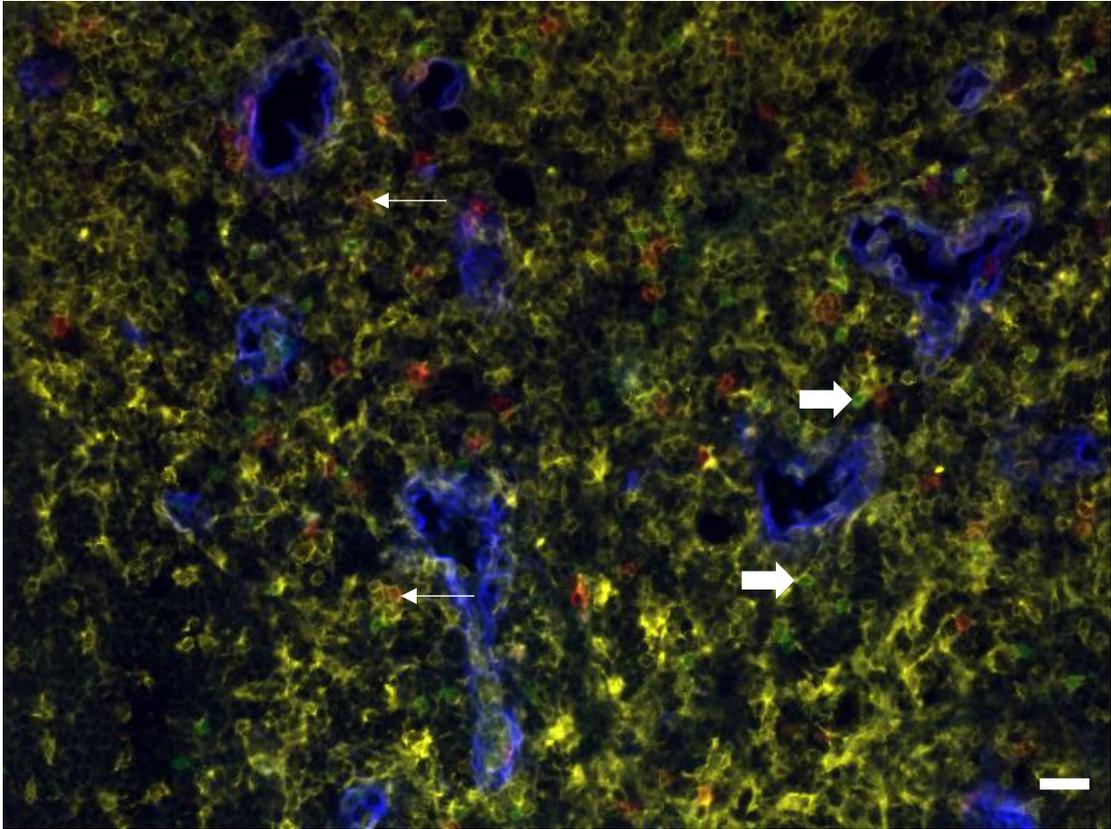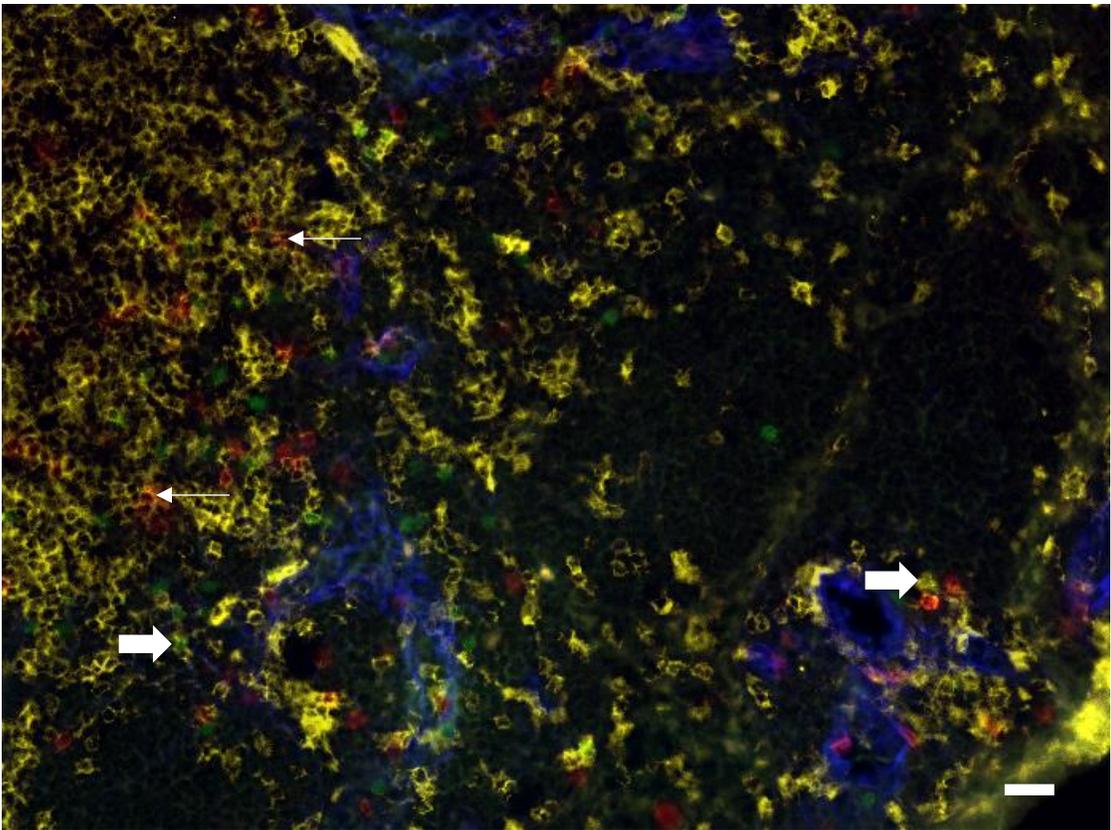
Figure 9. Piceatannol treatment did not significantly affect the localization of CD4$^+$ or CD8$^+$ T cells in the PLN. A) Representative image of CD4$^+$ T cells in an immunized PLN after piceatannol-treated cells were allowed to migrate for 1 hour. B) Representative image of CD8$^+$ T cells in an immunized PLN after piceatannol-treated cells were allowed to migrate for 1 hour (Blue=HEV, Green=CFSE$^+$ cells (treated), Red= Biotin$^+$ cells (untreated), Yellow=CD4$^+$ or CD8$^+$ cells for A and B, respectively). Thin arrows indicate the presence of transferred subtype$^+$ and biotin$^+$ cells, and thick arrows indicate transferred subtype$^+$ and CFSE$^+$ cells. Scale bar represents 50 µm. Results are from 1 experiment.

Results of previous experiments suggested that T cells were transmigrating across the HEV faster in immunized PLN than T cells in the control PLN (Grailer, 2010). Therefore, a short-term adoptive transfer assay was performed to further examine this possibility. Cells were biotinylated, adoptively transferred into recipient mice immunized 3 days prior and allowed to migrate for 5 minutes instead of 1 hour after transfer. A representative image of the 5-minute transfer is shown in Figure 10A. As seen in the image, the labeling was very clean and specific allowing for easy quantification of the number of transferred cells located inside versus outside of the HEV. Figure 10B shows the number of biotin$^+$ cells per 1,000 µm^2 area of HEV. As expected for such a short migration time, the majority of the transferred cells were located inside of the HEV. Furthermore, in this experiment there was no increase in the number of transferred cells located outside of the HEV in the immunized lymph nodes compared to the control tissues. Therefore, these initial results do not support the idea that CD4$^+$ or CD8$^+$ T cells cross the HEV into the PLN faster during an immune response.

A
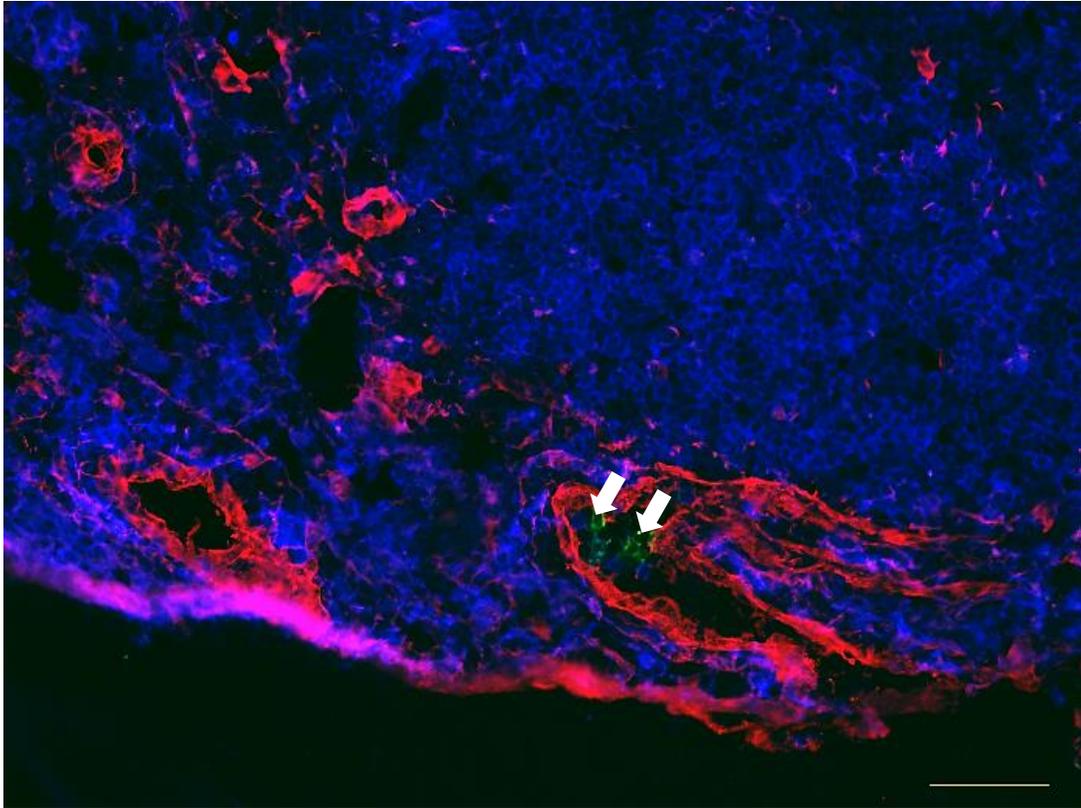
B
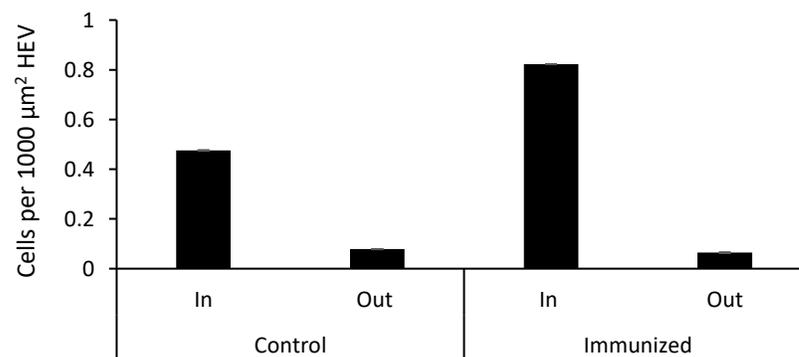
Figure 10. CD4⁺ or CD8⁺ T cells do not cross the HEV faster in immunized PLN. A) Representative image

of labeling in lymph node after adoptively transferred cells were allowed to migrate for 5 minutes; Blue=

CD4⁺ cells; Red= HEV; Green= biotin⁺ cells. Arrows indicate biotin⁺ transferred cells within the HEV. All

HEV within a tissue section were scored for biotin⁺ cells. Scale bar represents 50 μm. B) Graph of biotin⁺

cells per 1000 μm^2 of HEV in the immunized or control sections. Results are pooled from two sections made from one transfer experiment.

Discussion

Overall my work found that the differential migration of CD4+ and CD8+ T cells to immunized peripheral lymph nodes was not dependent on ZAP70 or PI3K signaling. In addition, ZAP70 and PI3K were not required for proper localization in the PLN or spleen. CD4$^+$ and CD8$^+$ T cell migration to the immunized lymph nodes was shown to be dependent on Gα_i signaling similarly to the control lymph nodes. It was also shown that CD4$^+$ or CD8$^+$ T cells do not cross the HEV faster in immunized lymph nodes.

Piceatannol treatment of splenic cells significantly reduced CD8$^+$ T cell migration to the spleen for mice that were allowed to respond to immunization for 3 and 7 days. This could be due to the piceatannol reducing the signaling downstream of the T cell receptor (TCR). Piceatannol has been shown to downregulate p-Erk, p-Akt, and p-p38 specifically (Kim et al., 2015). Akt is well known to be involved in intracellular signaling pathways that affect adhesion molecules and receptors involved in lymphocyte migration (Knieke et al., 2012; Stombolic and Woodgett, 2006). Akt is also known to phosphorylate proteins involved in cell polarization during migration (Enomoto et al., 2005). It is possible that piceatannol treatment of the cells affected their shape or deformability, which resulted in changes in circulation rates. However, this would not explain why CD4$^+$ T cell migration to the spleen was not reduced because the proteins mentioned are present in both cell types. Further, it is possible that the reduction in CD8$^+$ T cells found in the spleen was because they had increased migration to tissues not

sampled such as the lungs, liver, or mucosal lymphoid tissues. Future work could examine the amount of CD8^{+} T cells found in these tissues after piceatannol treatment and transfer.

Further, piceatannol's effect on localization of CD4^{+} and CD8^{+} T cells in the PLN and spleen were examined. Figures 8A, C, and 9A show that piceatannol treatment did not have a significant effect on the localization of CD4^{+} or CD8^{+} T cells. The quantitation of the ratio of cells In/Out of the splenic T cell zones showed that, although there was a slight increase in the In/Out ratio of both CD4^{+} and CD8^{+} T cells, there would likely not be a significant difference between the treated and untreated cells with more independent experiments done. Figures 9A-B show that there was not a large effect on the localization of piceatannol-treated cells in the PLN. This was determined by observing that there were no treated cells 'trapped' in the HEV of the PLN, and that the treated and untreated cells localized to similar areas once outside of the HEV. Quantifying the above observation in the similar ways as Figures 8A-C is complicated by the fact that there were no cells observed in the HEV after the 1-hour migration. However, it would be necessary to confirm the observations detailed above with quantitation of 3 independent experiments.

Piceatannol treatment has been found to reduce activation marker expression in activated CD8^{+} T cells (Kim et al., 2015). It has also been shown to reduce the transmigration of CD4^{+} T cells into resting lymph nodes in 30 minute migration experiments and block the L-selectin-mediated increase in T cell chemotaxis to CCL21 (Subramanian et al., 2012). In the present studies, the migration of lymphocytes to the PLN, either control or immunized, following 1 hour of migration was not significantly affected by piceatannol treatment. These pieces of data, along with Figure 8A, C, and 9A, suggest that ZAP70 does not play a major role in

the differential migration of CD4^{+} and CD8^{+} T cells during an immune response. Some groups

have found that ZAP70 plays a role in the directionality of T cell migration to chemokines *in*

vitro (Lin et al., 2010). It is possible that the T cells are able to compensate for the loss of ZAP70

signaling, and thus its role in integrin signaling, through synergy in the signaling pathways that

are stimulated by multiple different chemokines engaging the cell at the same time. This

cytokine 'milieu' could allow other pathways to compensate for the loss of one signal due to

piceatannol inhibition. Indeed, there are reports of different intracellular pathways being

activated depending on the chemokines, proteins, and T cell subtypes present (Schaeuble et al.,

2011). Also, several reports of synergy between, or among, various chemokine/receptor

networks have been reported (although the exact mechanism of such interaction networks has

been hard to disentangle) (Gouwy et al., 2011; Kuscher et al., 2009). The variables of

chemokine, chemokine receptor, cell type, and cell expression are a few of the parameters of

the cell migration formula. Although nascent, the development of high-throughput methods for

characterization of signaling pathway synergy with various perturbations has begun to unwind

complex networks such as chemokine signaling (Bendall et al., 2011). It would be interesting to

look for a possible synergy among pathways in piceatannol-treated cells, which allowed the

cells to compensate for loss of ZAP70 signaling by using a high-throughput method (e.x. single-

cell mass cytometry).

Previous studies using *in vitro* transwell migration assays had shown that wortmannin

treatment of cells does reduce migration to CCL21 (Subramanian, 2012). Given PI3K's

importance in signaling, it is surprising that wortmannin inhibition of PI3K did not affect CD4^{+} or

CD8^{+} T migration to the peripheral lymph nodes as shown in Figures 7A-B. Further,

quantification of spleen sections with wortmannin-treated or untreated cells (Figure 8B) showed that wortmannin treatment did not influence the localization of CD4^{+} or CD8^{+} T cells to splenic T cell areas. It is likely that wortmannin treatment of CD4^{+} and CD8^{+} T cells would not have a significant effect on localization in the PLN, although this was not examined. Some previous reports using wortmannin to inhibit PI3K proteins support this result (Matheu et al., 2007, Asperti-Boursin et al., 2007). As with Figure 6, the discrepancy could be explained by crosstalk compensation of the various signaling pathways and chemokines. It is possible that the cells can incorporate various other chemokine signaling and/or pathways to allow them to make up for the loss of pan-PI3K signaling due to wortmannin treatment. Importantly, Apsperti-Boursin and others found that cells treated with wortmannin at 100nM maintained PI3K inhibition for at least 2 hours. This adds support to the data in Figure 7 *in lieu* of western blot data of my own. Overall, these results support the idea that the mechanism for regulating the differential migration of CD4^{+} and CD8^{+} T cells during an immune response is not wholly dependent on ZAP70 and PI3K signaling.

Finally, results shown in Figure 10 suggest that CD4^{+} and CD8^{+} T cells do not cross the HEV significantly faster in immunized compared to control peripheral lymph nodes using 5-minute migration assays. However, it is possible that a 5-minute migration assay is simply too short for migration out of the HEV to occur in either tissue. A difference in migration between the resting and immunized PLN might be found if the cells were given a little more time to migrate across the HEV. A similar assay with a 10-minute migration time could address this question.

Future Directions and Conclusion

Follow up transfer assays with immunofluorescence microscopy should be done to quantitate the results qualitatively shown in Figure 9A-B. Although initial images from the first experiment suggest there is no difference in migration with piceatannol treatment at this time point, this should be confirmed. Interestingly, in Figure 9A-B there seemed to be fewer treated cells in the control peripheral lymph node images (CFSE$^+$ cells) compared to the immunized PLN. This result is not consistent with the data in Figure 6 that showed there was no reduction of CD4$^+$ or CD8$^+$ T cell migration to the control peripheral lymph node with piceatannol treatment. It is possible that the lack of CFSE$^+$ cells in the control peripheral lymph node was an artifact of the sectioning or labeling of the tissue. Labeling more sections from the same control peripheral lymph node tissue could confirm the result. Also, transfer and immunofluorescence imaging with wortmannin-treated cells would be a good follow up on Figure 9A-B.

The majority of groups that study T cell migration examine chemokine signaling as a large aspect of the migration 'equation'. It would be interesting to examine the dynamics of the cytokine 'milieu' and how it is affected by the immunization procedure used in our studies. Using a high-throughput Liquid Chromatography-Mass Spectroscopy approach could provide data that would tell us what chemokines are expressed differently in immunized mice compared to the unimmunized mice.

Opposite of chemokine expression are the cells that are sensing and responding to them. Examination of CD4$^+$ and CD8$^+$ T cell gene expression and/or transcriptome could elucidate some differences in intracellular responses to cytokine exposure that might help

explain the differential migration. Indeed, some groups have used high-throughput, 'systems' methods to examine the intracellular signaling that takes place before cell activation (Hat et al., 2011, Bordbar et al., 2012, De Simone et al., 2016). Multicolor fluorescence associated cell sorting with rtPCR on the single-cell populations would be a good method to look at expression of chemokine receptors and/or gene expression in response to chemokine exposure. Those methods in conjunction could hint at which chemokine signaling pathways to focus on with inhibitors or gene knockouts to tease apart the differential migration.

The data shown and discussed in this work, although not conclusive, has eliminated possibilities for the observed differential migration of CD4$^+$ and CD8$^+$ T cells during an immune response and suggested new possibilities. A better understanding of the migration mechanisms used by T cells could allow design of T cells with improved migration to tumor sites, as has been a noted issue for some immunotherapeutic regimens (Sackstein et al., 2017). This knowledge could also add to the development of immunotherapies for autoimmune diseases (Pozsgay et al., 2017). In all, this work adds to the ever-growing knowledge of T cell migration and, in the future, will hopefully be useful for therapies that help patients' lives.

References

Abernethy, N.J., Hay, J.B., Kimpton, W.G., Washington, E.A., and Cahill, R.N. (1990). Non-random recirculation of small, CD4+ and CD8+ T lymphocytes in sheep: evidence for lymphocyte subset-specific lymphocyte- endothelial cell recognition. Int. Immunol. *2*, 231–238.

Allfrey, V.G., Faulkner, R., and Mirsky, A.E. (1964). Acetylation and methylation of histones and their possible role in the regulation of rna synthesis. PNAS *51*, 786–794.

Asperti-Boursin, F., Real, E., Bismuth, G., Trautmann, A., and Donnadieu, E. (2007). CCR7 ligands control basal T cell motility within lymph node slices in a phosphoinositide 3–kinase– independent manner. J. Exp. Med. *204*, 1167–1179.

Bellone, M., and Calcinotto, A. (2013). Ways to enhance lymphocyte trafficking into tumors and fitness of tumor infiltrating lymphocytes. Front. Oncol. *3*.

Bendall, S.C., Simonds, E.F., Qiu, P., Amir, E.D., Krutzik, P.O., Finck, R., Bruggner, R.V., Melamed, R., Trejo, A., Ornatsky, O.I., et al. (2011). Single-cell mass cytometry of differential immune and drug responses across a human hematopoietic continuum. Science *332*, 687–696.

Blattman, J.N., Antia, R., Sourdive, D.J.D., Wang, X., Kaech, S.M., Murali-Krishna, K., Altman, J.D., and Ahmed, R. (2002). Estimating the precursor frequency of naive antigen-specific CD8 T cells. J. Exp. Med. *195*, 657–664.

Bluestone, J.A., Buckner, J.H., Fitch, M., Gitelman, S.E., Gupta, S., Hellerstein, M.K., Herold, K.C., Lares, A., Lee, M.R., Li, K., et al. (2015). Type 1 diabetes immunotherapy using polyclonal regulatory T cells. Sci. Transl. Med. *7*, 315ra189-315ra189.

Boettner, B., and Van Aelst, L. (2009). Control of cell adhesion dynamics by Rap1 signaling. Curr. Opin. in Cell Bio. *21*, 684–693.

Bordbar, A., Mo, M.L., Nakayasu, E.S., Schrimpe-Rutledge, A.C., Kim, Y.-M., Metz, T.O., Jones, M.B., Frank, B.C., Smith, R.D., Peterson, S.N., et al. (2012). Model-driven multi-omic data analysis elucidates metabolic immunomodulators of macrophage activation. Mol. Syst. Biol. *8*, 558.

Butterfield, L.H. (2013). Dendritic cells in cancer immunotherapy clinical trials: are we making progress? Front. Immunol. *4*.

Butterfield, L.H. (2015). Cancer vaccines. BMJ *350*.

Chan, A.C., Iwashima, M., Turck, C.W., and Weiss, A. (1992). ZAP-70: a 70 kd protein-tyrosine kinase that associates with the TCR zeta chain. Cell *71*, 649–662.

Chan, A.C., Kadlecek, T.A., Elder, M.E., Filipovich, A.H., Kuo, W.L., Iwashima, M., Parslow, T.G., and Weiss, A. (1994). ZAP-70 deficiency in an autosomal recessive form of severe combined immunodeficiency. Science *264*, 1599–1601.

Chen, A., Engel, P., and Tedder, T.F. (1995). Structural requirements regulate endoproteolytic release of the L-selectin (CD62L) adhesion receptor from the cell surface of leukocytes. J. Exp. Med. *182*, 519–530.

Critchley, D.R. (2004). Cytoskeletal proteins talin and vinculin in integrin-mediated adhesion. Biochem. Soc. Trans. *32*, 831–836.

Dai, H., Wang, Y., Lu, X., and Han, W. (2016). chimeric antigen receptors modified t-cells for cancer therapy. J. Natl. Cancer. Inst. *108*.

Day, C.E., Guillen, C., Willars, G.B., and Wardlaw, A.J. (2010). Characterization of the migration of lung and blood T cells in response CXCL12 in a three-dimensional matrix. Immunology *130*, 564–571.

De Simone, M., Arrigoni, A., Rossetti, G., Gruarin, P., Ranzani, V., Politano, C., Bonnal, R.J.P., Provasi, E., Sarnicola, M.L., Panzeri, I., et al. (2016). Transcriptional landscape of human tissue lymphocytes unveils uniqueness of tumor-infiltrating t regulatory cells. Immunity *45*, 1135–1147.

Diaz, C.M., Chiappori, A., Aurisicchio, L., Bagchi, A., Clark, J., Dubey, S., Fridman, A., Fabregas, J.C., Marshall, J., Scarselli, E., et al. (2013). Phase 1 studies of the safety and immunogenicity of electroporated HER2/CEA DNA vaccine followed by adenoviral boost immunization in patients with solid tumors. J. Transl. Med. *11*, 62.

Enomoto, A., Murakami, H., Asai, N., Morone, N., Watanabe, T., Kawai, K., Murakumo, Y., Usukura, J., Kaibuchi, K., and Takahashi, M. (2005). Akt/PKB regulates actin organization and cell motility via Girdin/APE. Dev. Cell *9*, 389–402.

Finlay, D.K., Rosenzweig, E., Sinclair, L.V., Feijoo-Carnero, C., Hukelmann, J.L., Rolf, J., Panteleyev, A.A., Okkenhaug, K., and Cantrell, D.A. (2012). PDK1 regulation of mTOR and hypoxia-inducible factor 1 integrate metabolism and migration of CD8+ T cells. J. Exp. Med. *209*, 2441–2453.

Gouwy, M., Struyf, S., Berghmans, N., Vanormelingen, C., Schols, D., and Damme, J.V. (2011). CXCR4 and CCR5 ligands cooperate in monocyte and lymphocyte migration and in inhibition of dual-tropic (R5/X4) HIV-1 infection. Eur. J. Immunol. *41*, 963–973.

Grailer, J.J. (2010). Differences in lymphocyte subset recruitment by anatomically distinct lymphoid tissues during homeostasis and inflammation. University of Wisconsin-Milwaukee.

Grailer, J.J., Kodera, M., and Steeber, D.A. (2009). L-selectin: Role in regulating homeostasis and cutaneous inflammation. J. Dermatol. Sci. *56*, 141–147.

Griffith, J.W., Sokol, C.L., and Luster, A.D. (2014). Chemokines and chemokine receptors: positioning cells for host defense and immunity. Annu. Rev. Immunol. *32*, 659–702.

Harris, E.S., Weyrich, A.S., and Zimmerman, G.A. (2013). Lessons from rare maladies: leukocyte adhesion deficiency syndromes. Curr. Opin. Hematol, *20*, 16–25.

Hat, B., Kazmierczak, B., and Lipniacki, T. (2011). B cell activation triggered by the formation of the small receptor cluster: a computational study. PLoS. Comput. Biol. *7*, e1002197.

Hervouet, E. (2018). The promising role of new generation HDACis in anti-cancer therapies. EBioMedicine *32*, 6–7.

Hwang, W.-T., Adams, S.F., Tahirovic, E., Hagemann, I.S., and Coukos, G. (2012). Prognostic significance of tumor-infiltrating T cells in ovarian cancer: A meta-analysis. Gynecol. Oncol. *124*, 192–198.

Jarmin, S.J., David, R., Ma, L., Chai, J.-G., Dewchand, H., Takesono, A., Ridley, A.J., Okkenhaug, K., and Marelli-Berg, F.M. (2008). T cell receptor–induced phosphoinositide-3-kinase p110δ activity is required for T cell localization to antigenic tissue in mice. J. Clin. Invest. *118*, 1154–1164.

Kershaw, M.H., Westwood, J.A., Parker, L.L., Wang, G., Eshhar, Z., Mavroukakis, S.A., White, D.E., Wunderlich, J.R., Canevari, S., Rogers-Freezer, L., et al. (2006). A Phase I study on adoptive immunotherapy using gene-modified t cells for ovarian cancer. Clin. Cancer. Res. *12*, 6106–6115.

Kim, D.-H., Lee, Y.-G., Park, H.-J., Lee, J.-A., Kim, H.J., Hwang, J.-K., and Choi, J.-M. (2015). Piceatannol inhibits effector T cell functions by suppressing TcR signaling. Int. J. Immunopharmacol. *25*, 285–292.

Kimpton, W.G., Washington, E.A., and Cahill, R.N. (1990). Non-random migration of CD4+, CD8+, gamma delta + T19+, and B cells between blood and lymph draining ileal and prescapular lymph nodes in the sheep fetus. Int. Immunol. *2*, 937–943.

Knieke, K., Lingel, H., Chamaon, K., and Brunner-Weinzierl, M.C. (2012). Migration of Th1 Lymphocytes Is Regulated by CD152 (CTLA-4)-Mediated Signaling via PI3 Kinase-Dependent Akt Activation. PLOS ONE *7*, e31391.

Kuscher, K., Danelon, G., Paoletti, S., Stefano, L., Schiraldi, M., Petkovic, V., Locati, M., Gerber, B.O., and Uguccioni, M. (2009). Synergy-inducing chemokines enhance CCR2 ligand activities on monocytes. Eur. J. Immunol. *39*, 1118–1128.

Ley, K., Laudanna, C., Cybulsky, M.I., and Nourshargh, S. (2007). Getting to the site of inflammation: the leukocyte adhesion cascade updated. Nat. Rev. Immunol. *7*, 678–689.

Lin, Y.-P., Cheng, Y.-J., Huang, J.-Y., Lin, H.-C., and Yang, B.-C. (2010). Zap70 controls the interaction of talin with integrin to regulate the chemotactic directionality of T-cell migration. Mol. Immunol. *47*, 2022–2029.

Luster, A.D., Alon, R., and von Andrian, U.H. (2005). Immune cell migration in inflammation: present and future therapeutic targets. Nat. Immunol. *6*, 1182–1190.

Mackay, C.R., Kimpton, W.G., Branon, M., and Cahill, R.N. (1988). Lymphocyte subsets show marked differences in their distribution between blood and the afferent and efferent lymph of peripheral lymph nodes. J. Exp. Med. *167*, 1755–1765.

Mandl, J.N., Liou, R., Klauschen, F., Vrisekoop, N., Monteiro, J.P., Yates, A.J., Huang, A.Y., and Germain, R.N. (2012). Quantification of lymph node transit times reveals differences in antigen surveillance strategies of naïve CD4+ and CD8+ T cells. Proc. Natl. Acad. Sci. U S A *109*, 18036–18041.

Martin, A.L., Schwartz, M.D., Jameson, S.C., and Shimizu, Y. (2008). Selective regulation of CD8 effector T cell migration by the p110γ isoform of phosphatidylinositol 3-kinase. J. Immunol. *180*, 2081–2088.

Matheu, M.P., Deane, J.A., Parker, I., Fruman, D.A., and Cahalan, M.D. (2007). Class IA phosphoinositide 3-kinase modulates basal lymphocyte motility in the lymph node. J. Immunol. *179*, 2261–2269.

Milone, M.C., Fish, J.D., Carpenito, C., Carroll, R.G., Binder, G.K., Teachey, D., Samanta, M., Lakhal, M., Gloss, B., Danet-Desnoyers, G., et al. (2009). Chimeric receptors containing CD137 signal transduction

domains mediate enhanced survival of T Cells and increased antileukemic efficacy in vivo. Mol. Ther. *17*, 1453–1464.

Morgan, R.A., Dudley, M.E., Wunderlich, J.R., Hughes, M.S., Yang, J.C., Sherry, R.M., Royal, R.E., Topalian, S.L., Kammula, U.S., Restifo, N.P., et al. (2006). Cancer regression in patients after transfer of genetically engineered lymphocytes. Science *314*, 126–129.

Murias, M., Jäger, W., Handler, N., Erker, T., Horvath, Z., Szekeres, T., Nohl, H., and Gille, L. (2005). Antioxidant, prooxidant and cytotoxic activity of hydroxylated resveratrol analogues: structure–activity relationship. Biochem. Pharmacol. *69*, 903–912.

Nicholson, M.W., Barclay, A.N., Singer, M.S., Rosen, S.D., and Merwe, P.A. van der (1998). affinity and kinetic analysis of L-selectin (CD62L) binding to glycosylation-dependent cell-adhesion molecule-1. J. Biol. Chem. *273*, 763–770.

Nombela-Arrieta, C., Mempel, T.R., Soriano, S.F., Mazo, I., Wymann, M.P., Hirsch, E., Martínez-A., C., Fukui, Y., von Andrian, U.H., and Stein, J.V. (2007). A central role for DOCK2 during interstitial lymphocyte motility and sphingosine-1-phosphate–mediated egress. J. Exp. Med. *204*, 497–510.

Pollizzi, K.N., and Powell, J.D. (2015). Regulation of T cells by mTOR: the known knowns and the known unknowns. Trends Immunol. *36*, 13–20.

Powell, J.D., Pollizzi, K.N., Heikamp, E.B., and Horton, M.R. (2012). Regulation of immune responses by mTOR. Ann. Rev. Immunol. *30*, 39–68.

Pozsgay, J., Szekanecz, Z., and Sármay, G. (2017). Antigen-specific immunotherapies in rheumatic diseases. Nat. Rev. Rheumatol.

Priddle, H., Hemmings, L., Monkley, S., Woods, A., Patel, B., Sutton, D., Dunn, G.A., Zicha, D., and Critchley, D.R. (1998). Disruption of the Talin gene compromises focal adhesion assembly in undifferentiated but not differentiated embryonic stem cells. J. Cell. Biol. *142*, 1121–1133.

Rosen, S.D. (2004). Ligands for L-Selectin: Homing, Inflammation, and Beyond. Ann. Rev. Immunol. *22*, 129–156.

Sackstein, R., Schatton, T., and Barthel, S.R. (2017). T-lymphocyte homing: an underappreciated yet critical hurdle for successful cancer immunotherapy. Lab. Invest. *97*, 669–697.

Schaeuble, K., Hauser, M.A., Singer, E., Groettrup, M., and Legler, D.F. (2011). Cross-talk between TCR and CCR7 signaling sets a temporal threshold for enhanced T lymphocyte migration. J. Immunol. *187*, 5645–5652.

Scimone, M.L., Felbinger, T.W., Mazo, I.B., Stein, J.V., Andrian, U.H. von, and Weninger, W. (2004). CXCL12 mediates CCR7-independent homing of central memory cells, but not naive T Cells, in peripheral lymph nodes. J. Exp. Med. *199*, 1113–1120.

Seto, E., and Yoshida, M. (2014). Erasers of histone acetylation: the histone deacetylase enzymes. Cold Spring Harb Perspect Biol *6*, a018713.

Sinclair, L.V., Finlay, D., Feijoo, C., Cornish, G.H., Gray, A., Ager, A., Okkenhaug, K., Hagenbeek, T.J., Spits, H., and Cantrell, D.A. (2008). Phosphatidylinositol-3-OH kinase and nutrient-sensing mTOR pathways control T lymphocyte trafficking. Nat. Immunol. *9*, 513–521.

Smith, M., Peterson, B., and Nelsen, B. (2016). Unlocking the therapeutic and commercial potential of CAR-T technology. Cell Gene Ther. Insights 2(3), 357-376

Soede, R.D.M., Wijnands, Y.M., Van Kouteren-Cobzaru, I., and Roos, E. (1998). ZAP-70 tyrosine kinase is required for LFA-1–dependent T cell migration. J. Cell Biol. *142*, 1371–1379.

Stambolic, V., and Woodgett, J.R. (2006). Functional distinctions of protein kinase B/Akt isoforms defined by their influence on cell migration. Trends Cell. Biol. *16*, 461–466.

Steeber, D.A., Green, N.E., Sato, S., and Tedder, T.F. (1996). Humoral immune responses in L-selectin-deficient mice. J. Immunol. *157*, 4899–4907.

Subramanian, H., Grailer, J.J., Ohlrich, K.C., Rymaszewski, A.L., Loppnow, J.J., Kodera, M., Conway, R.M., and Steeber, D.A. (2012). Signaling through L-selectin mediates enhanced chemotaxis of lymphocyte subsets to secondary lymphoid tissue chemokine. J. Immunol. *188*, 3223–3236.

Syrovatkina, V., Alegre, K.O., Dey, R., and Huang, X.-Y. (2016). Regulation, signaling, and physiological functions of G-Proteins. J. Mol. Bio. *428*, 3850–3868.

Thomas, M.S., Mitchell, J.S., DeNucci, C.C., Martin, A.L., and Shimizu, Y. (2008). The p110γ isoform of phosphatidylinositol 3-kinase regulates migration of effector CD4 T lymphocytes into peripheral inflammatory sites. J. Leukoc. Biol. *84*, 814–823.

Tipu, H.N. (2017). Leukocyte adhesion deficiency type I: A rare primary immunodeficiency disorder. Pediatr. Allergy. Immunol. *28*, 303–305.

Turner, M.D., Nedjai, B., Hurst, T., and Pennington, D.J. (2014). Cytokines and chemokines: At the crossroads of cell signalling and inflammatory disease. Biochim. Biophys. Acta *1843*, 2563–2582.

Venturi, G.M., Tu, L., Kadono, T., Khan, A.I., Fujimoto, Y., Oshel, P., Bock, C.B., Miller, A.S., Albrecht, R.M., Kubes, P., et al. (2003). Leukocyte migration is regulated by L-Selectin endoproteolytic release. Immunity *19*, 713–724.

Ward, S.G., Westwick, J., and Harris, S. (2011). Sat-Nav for T cells: Role of PI3K isoforms and lipid phosphatases in migration of T lymphocytes. Immunology Letters *138*, 15–18.

Waugh, C., Sinclair, L., Finlay, D., Bayascas, J.R., and Cantrell, D. (2009). Phosphoinositide (3,4,5)-triphosphate binding to phosphoinositide-dependent kinase 1 regulates a protein kinase B/Akt signaling threshold that dictates t-cell migration, not proliferation. Mol. Cell. Biol. *29*, 5952–5962.

West, A.C., and Johnstone, R.W. (2014). New and emerging HDAC inhibitors for cancer treatment. J. Clin. Invest. *124*, 30–39.

Westin, J.R. (2014). Status of PI3K/Akt/mTOR pathway inhibitors in lymphoma. Clin. Lymphoma. Myeloma. Leuk. *14*, 335–342.

Wolter, F., Clausnitzer, A., Akoglu, B., and Stein, J. (2002). Piceatannol, a natural analog of resveratrol, inhibits progression through the s phase of the cell cycle in colorectal cancer cell lines. J. Nutr. *132*, 298–302.

Yano, H., Nakanishi, S., Kimura, K., Hanai, N., Saitoh, Y., Fukui, Y., Nonomura, Y., and Matsuda, Y. (1993). Inhibition of histamine secretion by wortmannin through the blockade of phosphatidylinositol 3-kinase in RBL-2H3 cells. J. Biol. Chem. *268*, 25846–25856.

Yap, T.A., Garrett, M.D., Walton, M.I., Raynaud, F., de Bono, J.S., and Workman, P. (2008). Targeting the PI3K–AKT–mTOR pathway: progress, pitfalls, and promises. Curr. Opin. Pharmacol. *8*, 393–412.

Appendix

Introduction

Deacetylation of histones by histone deacetylases (HDACs) has been implicated in regulation of gene expression for many years (Allfrey et al., 1964). The biochemical pathways and wider effects on gene regulation of HDACs have been uncovered since these initial studies in the 1960s (Seto and Yoshida, 2014). The role of HDACs in gene regulation has become even more appreciated with the advent of epigenetic studies in recent years. HDACs role(s) in cancer garnered interest from groups once more information became available about its role in gene regulation. HDAC inhibitors (HDACi) have been studied clinically because of this interest (West and Johnstone, 2014). There are four FDA-approved HDACi as of 2018 (Vorinostat™, Romidepsin™, Panobinostat™, Belinostat™) with strong interest in developing new HDACi as evidenced by the 608 on-going or completed clinical studies investigating HDACi (Hervouet, 2018; Clinicaltrials.gov). However, a lack of specificity, and intolerable levels of toxicity, has limited the development of HDACi outside of the currently approved inhibitors.

Toxicity issues with current HDACi and continued interest in the development of HDACi for cancer lead to the collaboration between the Hossain lab and Steeber lab. The Hossain lab had previously synthesized novel HDACi based on the chemical structure of Romidepsin™ (FK228). The modifications made by the Hossain group were designed to reduce the toxicity of the new HDACi by increasing their class specificity. The Hossain group had synthesized 12 structural variants, including addition of different functional groups, and termed the variants compound 1-6 (Cpd1-6) and Cpd1-6'. The Hossain group delivered batches of the purified

compounds to the Steeber lab for testing of the drugs *in vitro* as described below. The data

from the assays performed show that one of the compounds (Cpd1') reduced prostate cancer

(DU145 cells) viability and inhibited HDAC activity *in vitro*.

MTT assay

Cells were allowed to adhere for 24 hours at 37°C with 5% CO_2. Compound 1' (Cpd1'),

Compound 5 (Cpd5), FK228, and DMSO control concentrations were diluted in series with

supplemented DMEM. The media was aspirated off the 96 well plate and the drug, or control,

concentrations were added to the plate in triplicate. The cells were incubated with the drugs or

DMSO controls for 48 hours. The drug and control treatments were removed and 200 µg/mL 3-

(4,5-dimethylthiazol-2-yl)-2,5-diphenyltetrazolium bromide (MTT) (Research Products

International, Mount Prospect, IL) diluted in supplemented DMEM was added to each well.

Cells were incubated with the MTT for 4 hours at 37°C with 5% CO_2. The MTT solution was

aspirated off and 200 µL DMSO was added to each well. The plate was mixed on a rotator for 10

minutes at a moderate pace and then the wells were mixed with a pipettor to dissolve all the

MTT in each well. The plate was read at 570 nm with the reference wavelength at 690 nm on a

Molecular Devices Versamax plate reader (San Jose, CA). The reference wavelength absorbance

for each well was subtracted. The average for the triplicate blank wells was calculated and also

subtracted from each well. The % viability of each concentration was calculated by dividing the

average absorbance for each drug concentration by the DMSO control for that concentration

(average drug concentration absorbance/average DMSO control absorbance).

H3 Acetylation Assay

DU145 cells were cultured as above. Cells were counted and resuspended at 60,000 cells/mL in supplemented DMEM. 1mL of cells at 60,000 cells/mL were added to wells of a 24 well plate. The cells were allowed to adhere for 24 hours at 37°C with 5% CO_2. The media was aspirated and Cpd1' at 50, 5, or 0.5 µM concentrations, or DMSO controls, in supplemented DMEM were added to the wells in duplicate. The plate was incubated at 37°C with 5% CO_2 for 24 hours. Cells were fixed with 350-500 µL 4% paraformaldehyde for 10 minutes at room temperature after the 24-hour incubation. 400-500 µL Tris buffered saline with 0.1% Tween 20 and 1% Bovine Serum Albumin (TBS-T w/ 1% BSA) was added to each well for 1 hour at 4°C for permeabilization. TBST w/ 1% BSA was removed and 350 to 500 µL rabbit anti-acetyl-Histone H3 (Lys9/Lys14) antibody (Cell Signaling Technology, Danvers, MA) at a 1:2000 dilution in TBS-T w/1% BSA was added to each well. The primary antibody was incubated with the cells overnight at 4°C. The primary antibody was removed and goat anti-rabbit IgG AlexaFluor™ 488 (Jackson ImmunoResearch, West Grove, PA) at a 1:500 dilution was added to each well and incubated for 1.5 hours at 4°C. The plate was removed from 4°C and 350-500 µL DAPI at 0.3 µg/mL was added to each well. DAPI was incubated in dark at room temperature for 15 minutes. Finally, wells were imaged with the fluorescence microscope as described in the main article's Materials and Methods section.

Results

Cpd1' had anti-proliferative activity at 50 uM as shown in Figure 11A. There was a significant reduction in cellular proliferation at 50 µM compared to 5 µM. However, the activity

of Cpd1' did not extend past the 50 µM concentration. A single follow up experiment showed that Cpd1' had anti-proliferative effects down to about 20-30 µM concentrations (data not shown). The histone deacetylase inhibitor (HDACi) activity of Cpd1' was assayed by immunofluorescence labeling of the acetylated form of the histone H3 protein. The antibody labeling detected acetylated lysine 9 and lysine 14 on the H3 protein. Increased fluorescence would indicate that the compound was not allowing the deacetylation of the H3 protein and thus indicate HDACi activity for Cpd1'. Figure 11B shows that the 50 µM concentration of Cpd1' increased the acetylation of the H3 protein compared to the DMSO control in DU145 cells. This indicates that Cpd1' has HDACi activity. The increase of acetylation at the 50 µM dose

correlates with the significant decrease in proliferation at the 50 µM dose shown in Figure 11A. This suggests that Cpd1' is reducing cell proliferation via HDACi activity.

Cpd5 was tested with the same MTT procedure and concentrations as Cpd1'. Figure 12 shows that Cpd5 did not have detectable anti-proliferative effects on the DU145 cells as measured by % viability.
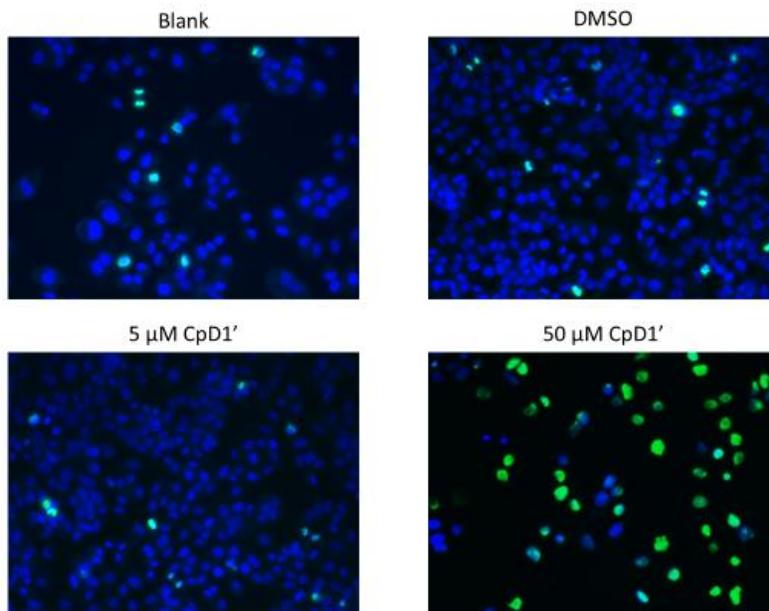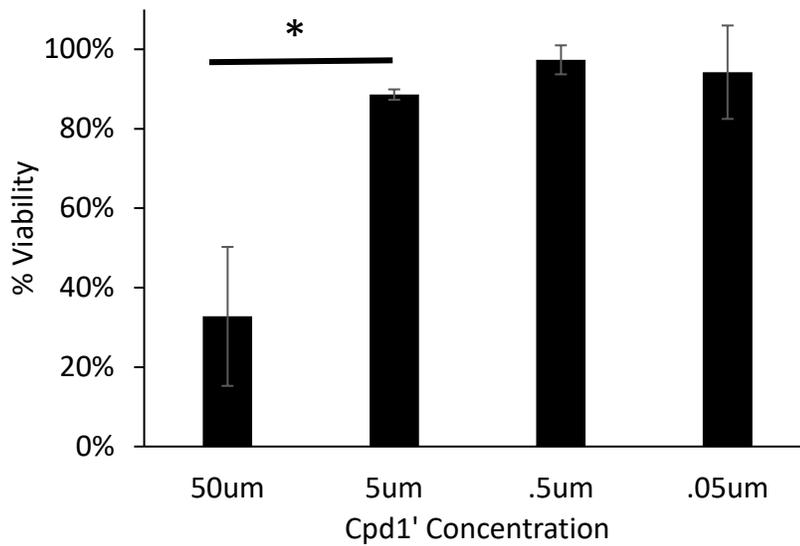
Green = acetylated H3   Blue = DAPI (nuclear stain)

Figure 11. Cpd1' significantly reduced DU145 cell viability after treatment for 48 hours and had histone deacetylase activity after 24 hours. A) DU145 cells were treated and MTT conversion was measured as above. The % viability was calculated as above. The 50 μM treatment results are from 3 independent experiments while the 5, 0.5, and 0.05 μM treatment results are from 2 independent experiments. Error bars indicate SEM. Asterisk above bar indicates significant difference between results at either end of bar. * $p < 0.05$ B) Representative images of histone H3 acetylation after treatment with DMSO or Cpd1'. Blue indicates nuclear staining by DAPI and Green indicates the presence of acetylated H3 histone.
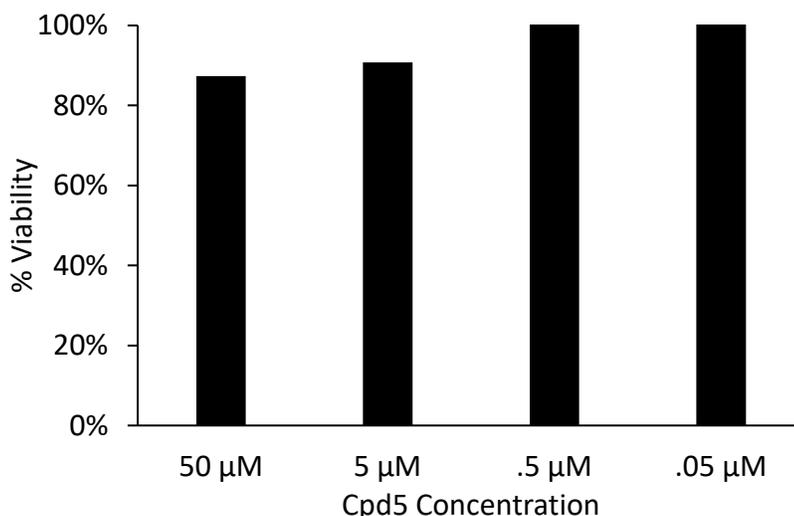
Figure 12. Cpd5 did not significantly reduce the % Viability of DU145 cells. The MTT assay was performed as described above with the concentrations shown. % viability was calculated as above. Results are from 1 experiment.

Discussion and Future Directions

Previous MTT assays with Cpd5 found that the compound significantly reduced DU145 cell proliferation at nanomolar concentrations. Figure 12 shows that there was no significant reduction in proliferation by Cpd5 even at the 50 μM concentration. This suggests that the

compound was not as active as it was in previous experiments. The FK228 positive control achieved reduction of proliferation in the previously reported nanomolar range (data not shown), and Cpd1' showed reduction in the micromolar range. Accordingly, it is not likely that differences in the MTT assay are to blame. It is possible that the synthesis and/or purification of the compound was not the same as in previous assays. Cpd5 received from Dr.Hossain's group will be tested with the MTT assay as described above until an active batch of the compound is found. Follow up MTT assays could also be done with Cpd1' to further define the effective range for the compound.

Figure 11B qualitatively shows that Cpd1' had strong HDACi activity at the 50 μM concentration. Preliminary testing was done on an assay using flow cytometry to quantitate the level of H3 acetylation. A quantitative measure of H3 acetylation would allow for stronger support of the conclusion that Cpd1' had significantly higher HDACi activity than the DMSO control. It would also further support the correlation between Cpd1's HDACi activity and anti-proliferative effects.

Pharmacokinetic studies of Cpd1' in mouse model(s) would be the next step in the consideration of the compound as a cancer therapeutic. Injecting Cpd1' intraperitoneally (i.p.) at a yet to be determined concentration (presumably in the mg/kg range) and sampling blood at 30-minute intervals via a retroorbital eye bleed procedure could be a good start to understanding the pharmacokinetics of the drug. It would also be interesting to sample various tissues (e.g. spleen, lymph nodes, kidney, heart, intestine) to examine the distribution of the drug in the mouse after injection. These tissues could be sampled from control and experimental mice at 12, 24, and 48 hours after i.p. injection of the drug as a first experiment.

Finally, a dosing study to examine the effectiveness of Cpd1' in a mouse tumor model would be necessary to show effectiveness *in vivo*. Cpd1' could be injected i.p. into mice bearing tumors. Female Balb/c mice bearing 4T1 tumors in their mammary fat pads to model stage IV breast cancer is a model used in the Steeber lab to examine myeloid-derived suppressor cell (MDSC) biology in tumors. It would be interesting to see the effects, if any, of Cpd1' on the growth of 4T1 tumors. Most 4T1 tumors are visible as a small bump at the injection site 2 weeks post injection. The pharmacokinetics data from the suggested experiments would be useful to set up the dosing plan, but an *a priori* plan could be to dose the mice with Cpd1' in the mg/kg range once weekly starting one week after tumor injection. Tumor area could be measured with calipers, and control versus treated tumors would be compared. It would be possible to inject the compound and control directly into the tumor if no effect is found with i.p. dosing to determine if the dosing was not high enough or if the compound is not effective *in vivo*.

These data shown, and future studies suggested, would provide more information on the effectiveness of Cpd1' *in vivo.* These efforts would hopefully show the compound to be an effective cancer therapeutic and be a viable option to help patients with the disease.